**Murdoch University**

**Division of Science and Engineering**

**PEC624**

**Master of Science in Renewable Energy**

**DISSERTATION**

**PV Systems with
Second Life Li-Ion Battery Technology**

**2012**

**By**          Chein Leung
**Submitted**:          June 2012

# DECLARATION

The work performed in this project is to the best of knowledge to the author that attributable to the author.  Where use is made of findings or results made by others they are appropriately referenced.

# ABSTRACT

Increasingly, PV self-consumption (PVSC) is becoming an important aspect of storing or deferring energy generated from distributed solar energy systems. Combined with the high specific energy capacities of lithium ion batteries, there is the potential of increasing the amount of solar energy that is consumed at the location where it is generated. The use of second-life lithium ion batteries in PVSC systems is a relatively new concept that is still undergoing active research within the scientific community.

Using second-life lithiated iron phosphate (LFP) batteries, this project models a PVSC environment with the HOMER program. The simulation results suggest that the amount of PVSC in an environment is contingent upon the available solar radiation and the demand for power. Also, the results indicate that there are no distinguishable differences in using new or second-life lithium ion batteries in a PVSC environment so long as they can withstand the frequent cycling induced by the variable availability of solar radiation and the random demand for power by residential loads. Attempts to quantify the effective utilization of solar power were also performed by calculating the PVSC factor from the simulation results.

# ACKNOWLEDGMENTS

# TABLE OF CONTENTS

# TABLES

# FIGURES

# Chapter 1: Introduction

## 1.1 Background

The concept of using battery technology to store and defer the consumption of solar power has been widely used in off-grid solar power applications including remote area power systems (RAPS) [1]. The current photovoltaic self-consumption (PVSC) systems that are being trialled explore the use of battery storage technologies in residential environments. Unlike RAPS, a permanent connection to the electricity grid is maintained to maximize the use of locally generated solar power whilst ensuring security in the supply of electricity to the user [2].

## 1.2 Research Objectives

This project is focussed on the use of second-life lithium ion batteries (LIB) in PVSC systems. The question that the project seeks to explore is whether or not the use of second-life LIBs impacts upon the level of PVSC within a residential environment. The main objectives of the project are to:

1. Introduce the concept of PVSC and review current PVSC systems using LIB technologies;

2. Review the electrochemical properties of LIBs;

3. Gain insight into the operation of PVSC systems using second-life LIBs by way of simulation; and to,

4. Explore the use of LIBs in PVSC systems under primary load conditions where the demand for power is served immediately and to compare this to situations where the load is actively managed.

## 1.3   Research Focus

Chapter 1 outlines the main research objectives and limitations of this project. Beyond this, Chapter 2 is the first part of the literature review that will introduce the concept of PVSC as it is known in the scientific community. As part of this review, three case studies of PVSC systems will be analysed to illustrate the current work in trialling PVSC systems in the community. The first one is an illustration of the PVSC concept from a network operator's perspective, featuring residential and community PVSC systems. In addition to this, the research reviews a residential PVSC system in Europe and the technologies that underpin the operation of the PVSC system. Finally, in the third example, the research investigates the concept of incorporating active demand side management into PVSC systems. This demonstration does not use LIBs, but the knowledge gained from such a demonstration could be applied to a PVSC system using LIBs.

Chapter 3 extends the literature review to summarize the key electrochemical properties of LIBs. LIBs with different anodes and cathodes have their own unique electrical profile and attempts are made to review the research performed on characterising their electrochemical behaviour. Additionally, information about the electrochemical performance of the lithiated iron phosphate (LFP) battery will also be provided in this

chapter. Chapter 4 illustrates the methodology used to develop the model and how information from the preceding chapters is incorporated in the simulation.

The results of the simulation and the insights gained from HOMER are documented in Chapter 5. The main insights arising from the simulation and some recommendations for further research work are presented in Chapter 6 as the report concludes.

## 1.4 Limitations

One of the key limitations of this project is that it will not be possible to validate the findings with respect to data from an actual PVSC system. To ensure that the model is accurate it would be necessary to validate the parameters for each component against experimental data. For the LIB model, this could mean testing the battery in a laboratory environment.

Although HOMER is a cost optimization program, the simulation is still able to provide insight into the power flows within a PVSC system. The possible limitation of this is that overall performance is based on the cost of energy produced rather than what would optimize the utilisation of the solar and battery systems in the PVSC system. In spite of this, the costs used in the model are based on realistic assumptions and, where possible, market values are used for the costs of goods and services.

Furthermore, there are currently few performance measures to describe the utilization of solar energy within a PVSC system. This can limit the ability to assess the accuracy of the

model and to ensure that all the factors that affect PVSC have been considered in the simulation.

# Chapter 2: Analytical Review of PV Self-Consumption

## 2.1 Background

A Photovoltaic Self-Consumption (PVSC) system is a system in which users generate solar energy for immediate or deferred consumption [2]. The ability to control how this energy is consumed enables the user to direct the generated energy to service a load or to store this in a battery system for later use. At present, sealed lead-acid, lithium-ion and zinc-bromine batteries are the most common types of batteries used in PVSC systems [3, 4].

In a PVSC system, use is made of energy control systems to direct the solar energy to service the load, to storage or to export to the external electricity grid. As well as being able to redistribute any extra power, the grid also allows electricity to be imported when there is insufficient power from the solar panels and the battery to service the load. In that sense, the energy management system monitors the available power in the PVSC system and in so doing switches between the power generated by the solar panels, the battery and the grid to service the load.

### 2.1.1 Impact on Grid Management

An important benefit of increasing PVSC is that it reduces the temporal peaks in the network load profile. Peak-shaving [5] occurs when the energy stored in the battery system can be used to service the load [6] and reduce the need for power from the grid to supply the load. Deferring the consumption of solar energy reduces the need for the network operator to invest in the spinning reserve that has traditionally been kept to serve

unexpected increases in load demand. Thus, increasing the level of PVSC at a local level can bring about significant benefits to the electricity network as a whole.

## 2.2 The Solar Smart Home Project

The Solar Smart Home Project (SSHP) is operated by the Sacramento Municipal Utility District (SMUD) in the USA with the objective of increasing the use of renewable energy in residential properties [4]. The project, jointly funded by the US Department of Energy and the SMUD, involves partnerships with organizations such as the National Renewable Energy Laboratory (NREL), GridPoint and Navigant Consulting [7]. Initially, the program resulted in 550 homes in the city of Anatolia, Sacramento being fitted with solar panels and built-in photovoltaic (BIPV) roof-slates. As illustrated in Table 1, the SSHP is an important component of SMUD's overall energy efficiency strategy.

**Table 1: SMUD Service District Profile**

| SMUD Service Area | Service Area Statistics |
|---|---|
|  | **Ownership Status:** Publicly owned utility.<br>**Population Serviced:** 1.4 million people.<br>**Current Energy Mix:**<br>• Biomass Energy: 81MW<br>• Solar Energy: 3,600MW<br>• Wind Energy: 2,30MW supplied by Solano Wind (Outside of SMUD Service District)<br>**Other Energy Programs:**<br>• Pumped Stored Hydro Program (400MW)<br>• Sacramento Solar Highways (1.4MW)<br>• Anatolia Smart Grid Pilot (600,000 meters)<br>• Plug-In Hybrid Electric Vehicle Infrastructure.<br>• Solar Smart Homes Project. |
| **Source: Microgrids: US Activities [8]** ||

In 2011 [9], as part of the SSHP program, 55 to 65 homes were connected to residential or community based battery storage systems to supplement the energy provided from the solar systems and the electricity grid [10]. Throughout the duration of the project, SMUD intends to investigate the best approach to integrate PVSC into the community, the impact this will have on the network and what influences households to increase PVSC [9].

### 2.2.1 Impact on SMUD Grid

A typical profile of the average daily load on the SMUD network is shown in Figure 1.
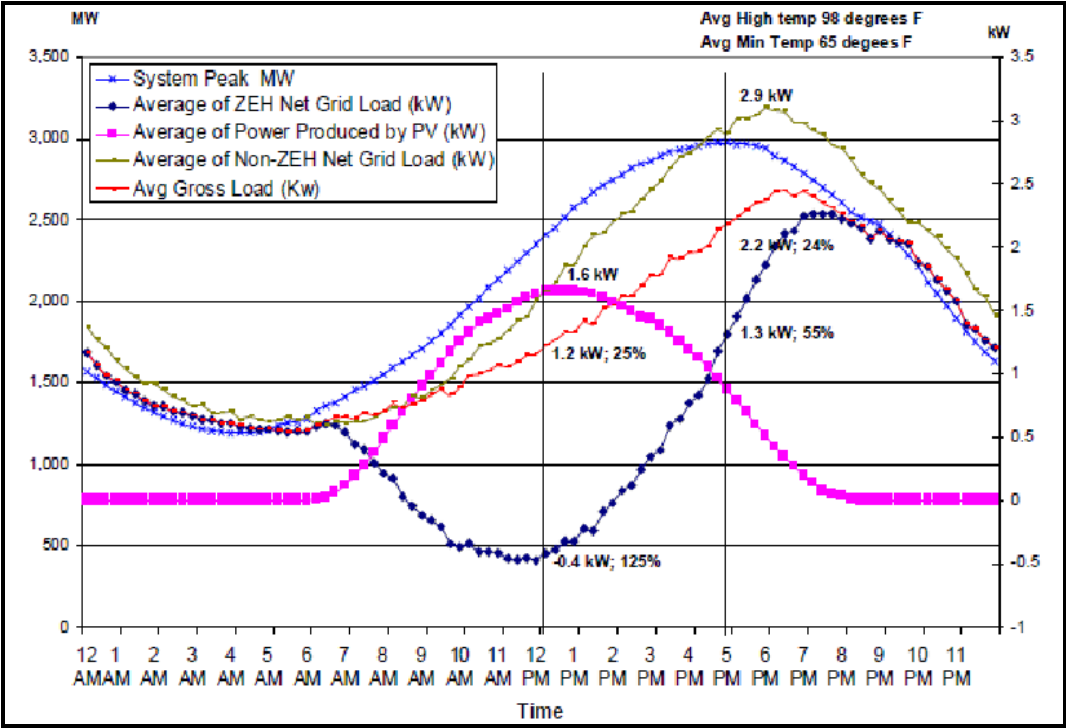


**Figure 1: Average Daily Load Profile of the SMUD Grid**
**Source: Utilities' Perspective of Energy Storage [11]**

The load profile shows two distinctive patterns. Firstly, the network operates on minimum load demand during the early hours of the day. Beyond this time, the load increases monotonically before levelling at its peak at about 3,000MW (at 5:00pm). At this point in time, the Zero Energy Homes (ZEH) imposes their demand for power from the grid. After reaching the maximum peak load of the day, the load then decreases monotonically back to a base load of about 1,250MW.

Secondly, the PV energy exported to the grid peaks during the middle of the day whilst providing no input when solar radiation drops to a minimum. Although this is

characteristic of the way in which solar power is made available to the grid [9], the peak solar output does not coincide with the peak load demand. As a result, the solar energy is not utilised and the network load is underserved. In this situation, a PVSC system can provide power to the householder and directly service their afternoon load demands by releasing stored energy from a battery system that has been continuously charging throughout the day.

### 2.2.2  Residential PVSC

A key milestone of the current project is to connect 34 residential properties into self contained PVSC systems. As illustrated in Figure 2, this system consists of grid-connected BIPV solar systems and an on-site lithium ion battery system. The solar system has a nominal capacity of 2kWh-4kWh [12] whilst the maximum capacity of the battery system is rated at 10kWh (with $LiNiO_2$ cathode) [13]. The power from these systems is directly coupled to the AC bus through an inverter system with a nominal capacity of 3.2kW [11].
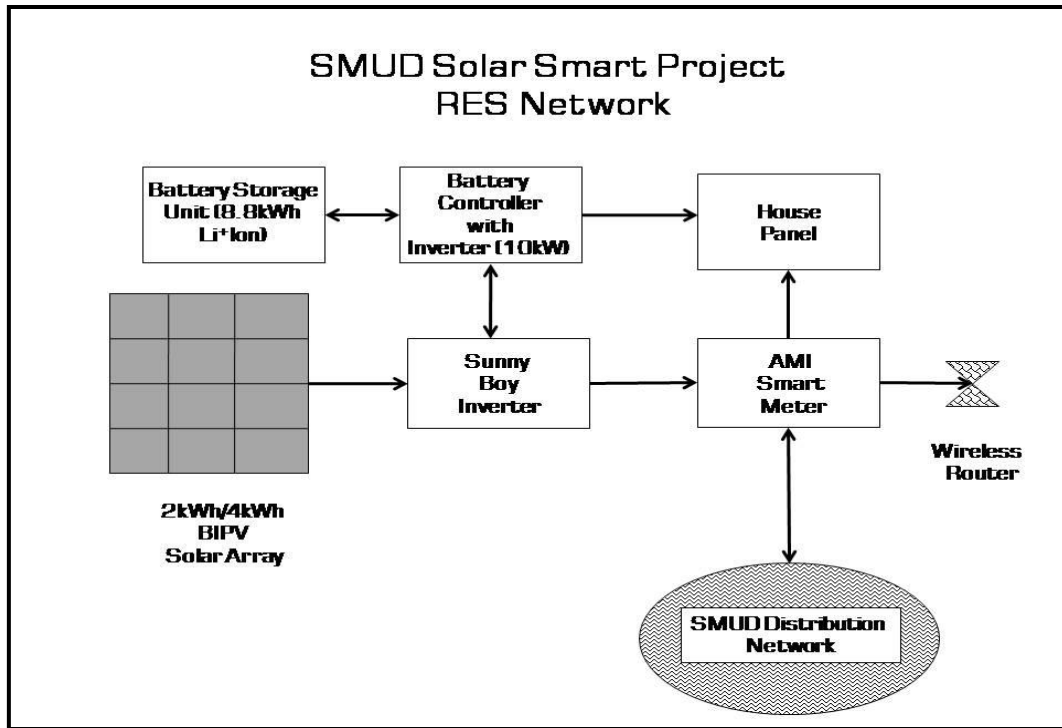
**Figure 2: Schematic Representation of a Residential Energy System**
**Source: Adapted From Utilities' Perspective of Energy Storage[11]**

During its operation, it is envisaged that each property will be monitored for the amount of PVSC that is occurring and the factors that encourage users to increase PVSC over exporting excess solar energy back to the grid [11]. The ability to export electricity back to the grid and to arbitrage on changes in the spot electricity price is one of the key incentives provided to households to increase their PVSC.

### 2.2.3 Community PVSC

The community PVSC system consists of a pad mounted battery system installed adjacent to the local distribution transformer. The battery system is scaled to have a capacity of 30kWh (with $LiNiO_2$ cathode) [13], providing 3 to 4 residential properties with energy

storage capabilities [4]. As shown in Figure 3, each household that is connected to a community PVSC unit is not required to retrofit their existing solar installations.
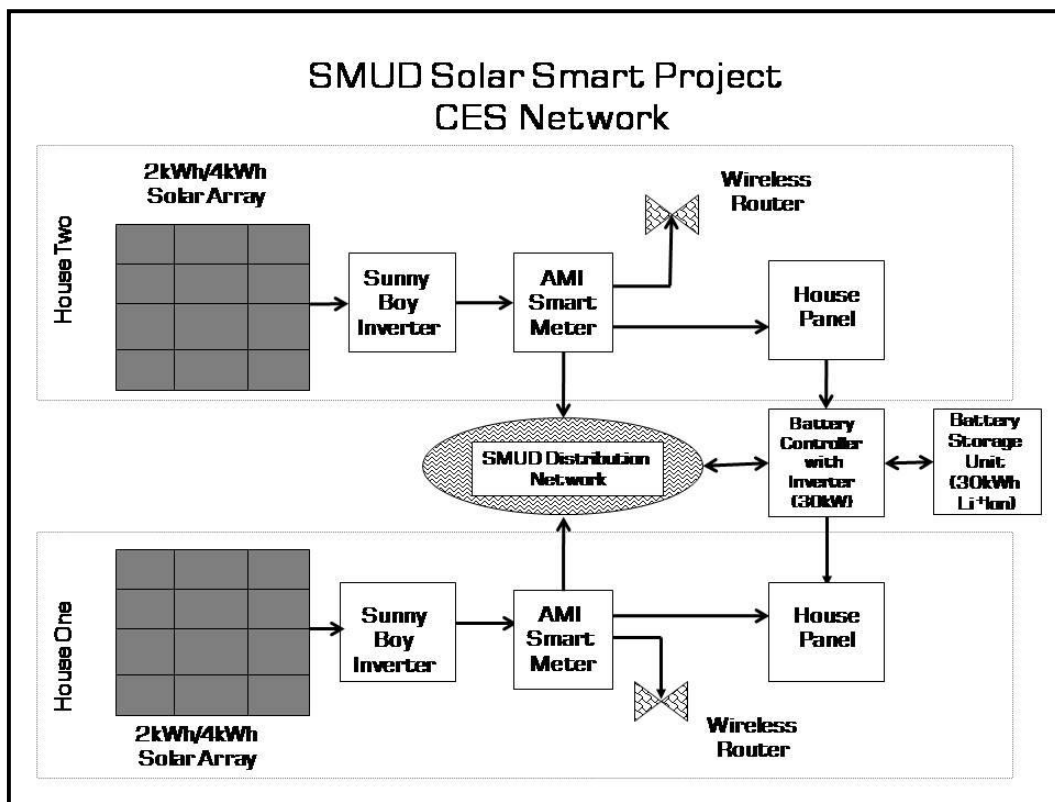


**Figure 3: Schematic Representation of a Community Energy System**
**Source: Adapted From Utilities' Perspective of Energy Storage[11]**

In a community PVSC system, issues regarding power reliability, power quality and system capacity are more salient [11] than for a residential PVSC system. In spite of this, transmission losses are kept to a minimum because the battery system is located at the local distribution feeder. On average, each household is still provided with the same amount of storage capacity as in the residential PVSC system, but the responsibility to maintain and monitor the system falls to the network operator. As such, sharing the power stored in the battery system allows temporal changes to domestic load demands to be served from a larger reservoir of stored solar energy.

### 2.2.4  Summary

The SMUD project illustrates the possibility of offering solar energy storage facilities in residential or community PVSC systems.  Whereas existing grid connected solar systems provides excess electricity back generated from the solar system back to the grid, the used of battery storage technology provides a means for excess energy to be stored and supplied to the load at a later time.  However, the integration of PVSC may provide some challenges to energy system designers.

Firstly, roof mounted BIPV roof slates may not necessarily be mounted in the direction of the azimuth or the Sacramento latitude thereby reducing the amount of solar energy that can be captured over a period of time and fed back into a PVSC system.  In addition to this, in both the residential and community PVSC systems, the size of the battery system is considerably larger than the peak output possible from the solar roof-slates.  This may be due to the fact that LIBs cannot be continuously deep-cycled and simultaneously uphold a high standard of performance.  Limiting the depth-of-discharge or the amount of current draw possible from the battery limits the amount of stored solar energy that can be used to power the load.

For community PVSC systems, it is necessary to design a system that can simultaneously serve the peak load demands of several households.  The community battery system is mounted adjacent to the local distribution feeder and is charged by the residential properties connected to the same distribution feeder that have roof mounted solar power systems.  However, issues of reactive power control from multiple sources of solar

installations and transmission and distribution losses would require systems to be designed in such a way as to maintain the network operator's standard of power quality and system integrity.

Conversely, the ease of connecting a household to a community PVSC system could be more attractive to having to retrofit an existing solar installation for PVSC. This scenario offers the opportunity for properties without a solar installation to be able to tap into the reservoir of solar energy stored in the community battery system.

## 2.3    The Sol-Ion Project

Beginning in 2008 [7], the Sol-Ion project is a joint initiative between Germany and France [14] to develop, install and study the use of LIB technology in residential PVSC systems [15]. With the objective of increasing solar power integration into the grid, changes in the German regulatory framework were made in 2010 [14] giving solar operators the right to a rebate for solar energy consumed in the "immediate vicinity of the installation" [16] from where it is produced. The companies involved in this project include Voltwerk Electronics, SAFT, Tenesol and E.ON Bayern [17] and research organizations like the Fraunhofer Institute, Institut National de I'Energie Solaire International Solar Energy Agency, Institute for Wind Energy and Energy System Technology and the Zentrum für Sonnenenergie und Wasserstoff-Forschung [17] with test sites being established in places such as Kassel, Germany and the French administrative unit of Guadeloupe.

### 2.3.1  System Specifications

As a consequence of these new regulations, each PVSC system must contain monitoring devices that can measure the amount of solar power exported to the grid and the amount of PVSC [18] of each household. Figure 4 illustrates the design of the PVSC system in the Sol-Ion project.
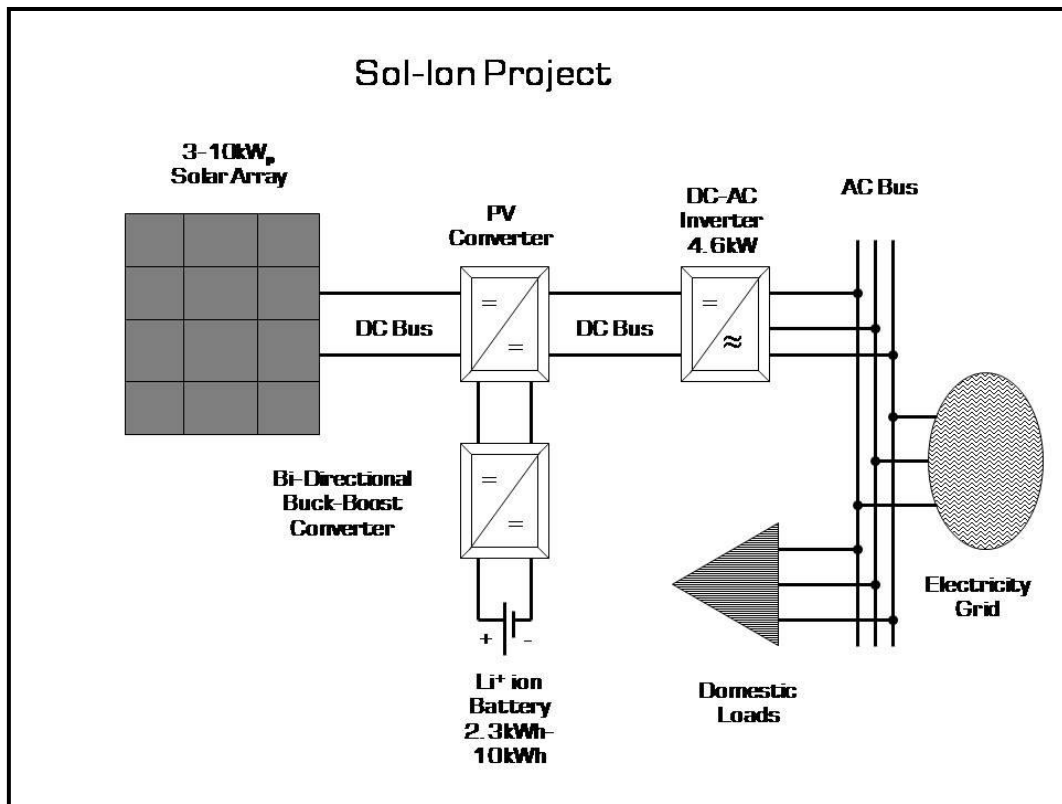


**Figure 4: Schematic Representation of the Sol-Ion PVSC System**
**Source: Adapted From Photovoltaic Self-Consumption In Germany Using Lithium-Ion Storage To Increase Self-Consumed Photovoltaic Energy [18]**

As illustrated in Figure 4, the Sol-Ion project seeks to study only residential PVSC systems.  In these systems, the size of the solar array varies between 3-10kWp [19]. Currently, only LIBs with capacities up to 10kWh (with $LiNiO_2$ cathode) [13] are being

trialled. The battery system is protected from damage by not discharging it by more than 60% of its nominal capacity [18] whilst the buck-boost converter is used to prevent overcharging or discharging of the battery system [18].

The buck-boost converter is commonly used in electric vehicles to control the flow of power when the vehicle regenerates power into the battery during braking and draws power from it when the vehicle motors [20]. In the PVSC system, the voltage bucks or decreases to the charge voltage of the battery and is boosted or increased to the DC bus voltage when required to power the load.

Also, in this PVSC system, the meters measure both the power flows between the solar system and the grid and the amount of power that is supplied from the system to the loads [21]. The purpose of measuring the actual amount of self consumed power is to not only measure the amount of locally consumed solar power but also as a way to furnish evidence for future claims for the rebate [16, 22].

### 2.3.2 The Sol-Ion PVSC System

Figure 5 shows a representative residential load profile in Europe. From inspection of the load profile, it can be seen that the load peaks for an extended period of time during the mornings and evenings. During this time, the PVSC system follows the load servicing it using solar power. The profile shows the ability of the PVSC system to service the load using solar power during the day and into the early evenings [23].
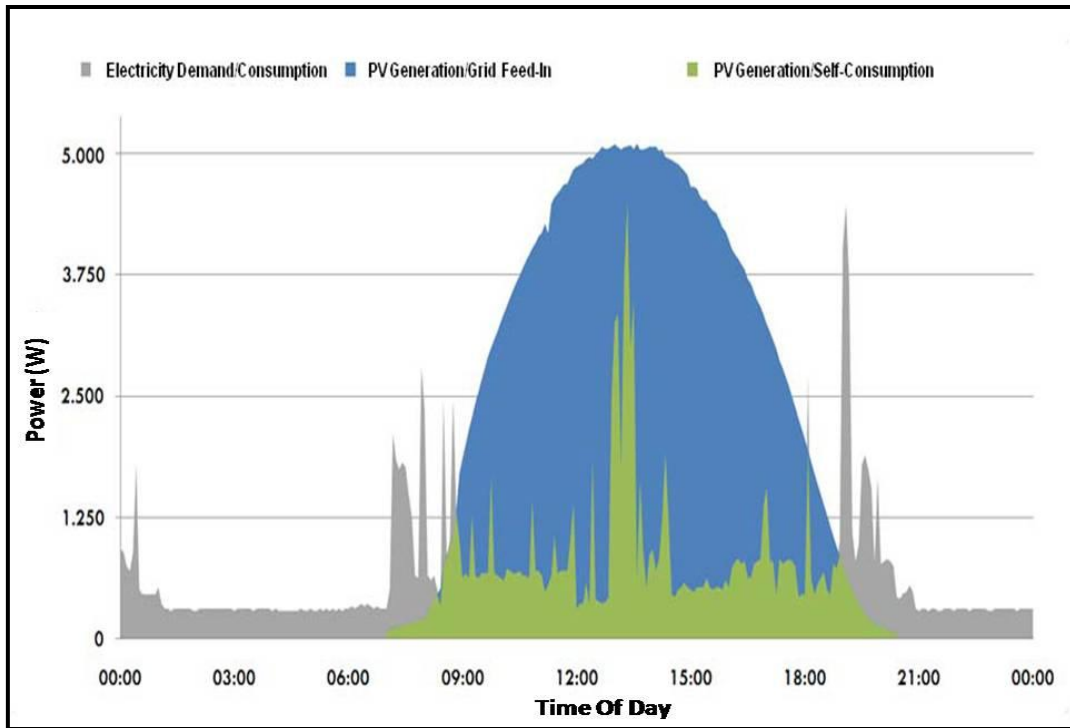
**Figure 5: Load Profile for Household in Kassel Germany**
**Source: From Self-Supply System Based on PV [23]**

Figure 6 illustrates the cycling behaviour of a LIB taken from the Guadeloupe [24] test site. It shows that 97% of the solar energy supplied to charge the battery system was consumed (142kWh) [24] over a period of a month.
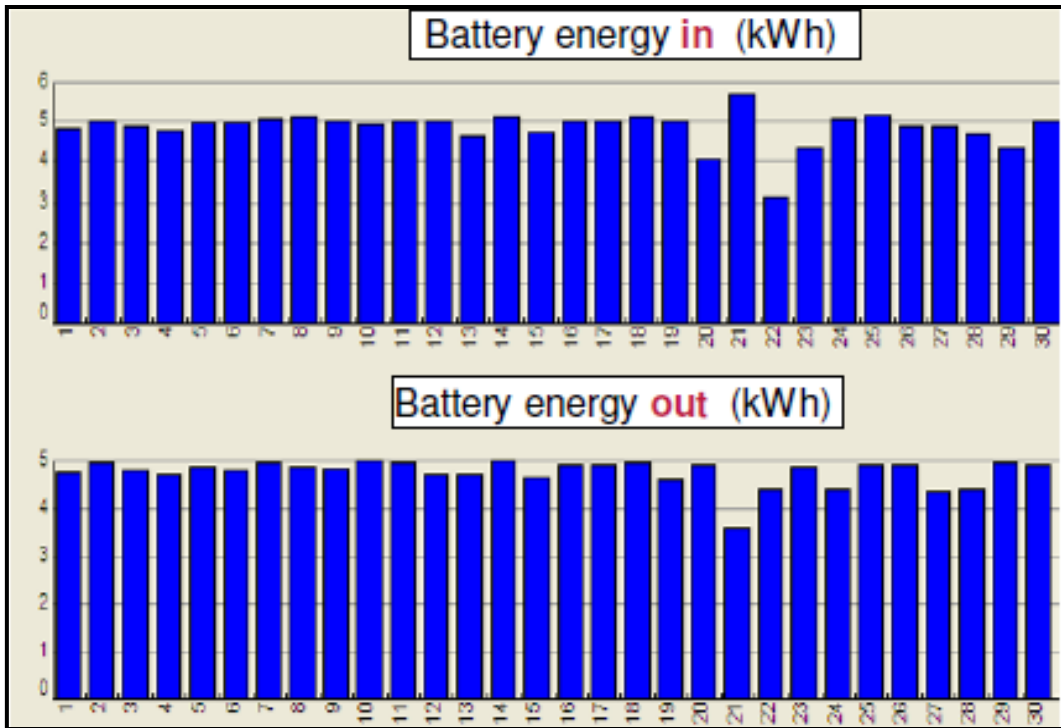
**Figure 6: Charge-Discharge Profile of Battery at Guadeloupe**
**Source: Residential PV Systems Combined with Energy Storage [24]**

At this site, the depth-of-discharge of the battery averaged about 45% [24], with between 5-6kWh of power cycled into and out of the battery [24]. For safety reasons, this ensures that the LIB, rated at 10kWh, is not over discharged.

### 2.3.3  Summary

The Sol-Ion project provides additional insight into the PVSC system's operating environment. In such a system, use is made of bi-directional buck-boost converters to regulate the charge and discharge of the battery and dual meters are used to monitor and measure the amount of PVSC. When compared to grid-connected solar installations, this adds to the functions that have to be performed by the PVSC system.

Results from the project have also provided insights into the operation of the battery. The charge-discharge profile provided from the Guadeloupe site illustrates the ongoing charging and discharging of the battery in the system. The battery system in the PVSC system is not conditioned to provide spinning reserve or back-up power, but rather, is an integral part of the power system that continuously supplies power to the load. The discharging of the battery to an average depth-of-discharge of 45-60% suggests that, for safety reasons, there is unused, idle capacity within this PVSC system. A LIB battery with an electrochemistry that has the propensity to tolerate deep discharging and a high tolerance to abuse conditions could increase the amount of PVSC in such a system.

## 2.4    The GEDELOS PVSC System

The GEDELOS PVSC system augments PVSC with active demand side management [25]. Instead of using LIBs, this PVSC system uses lead-acid batteries (LaBs). As illustrated in Figure 7, the PVSC system utilises a solar array rated at $7kW_p$ to support a LaB with a capacity of 72kWh. In this experimental model, the cycling of the LaB is determined by the availability of solar power and the active management of when the load is served.
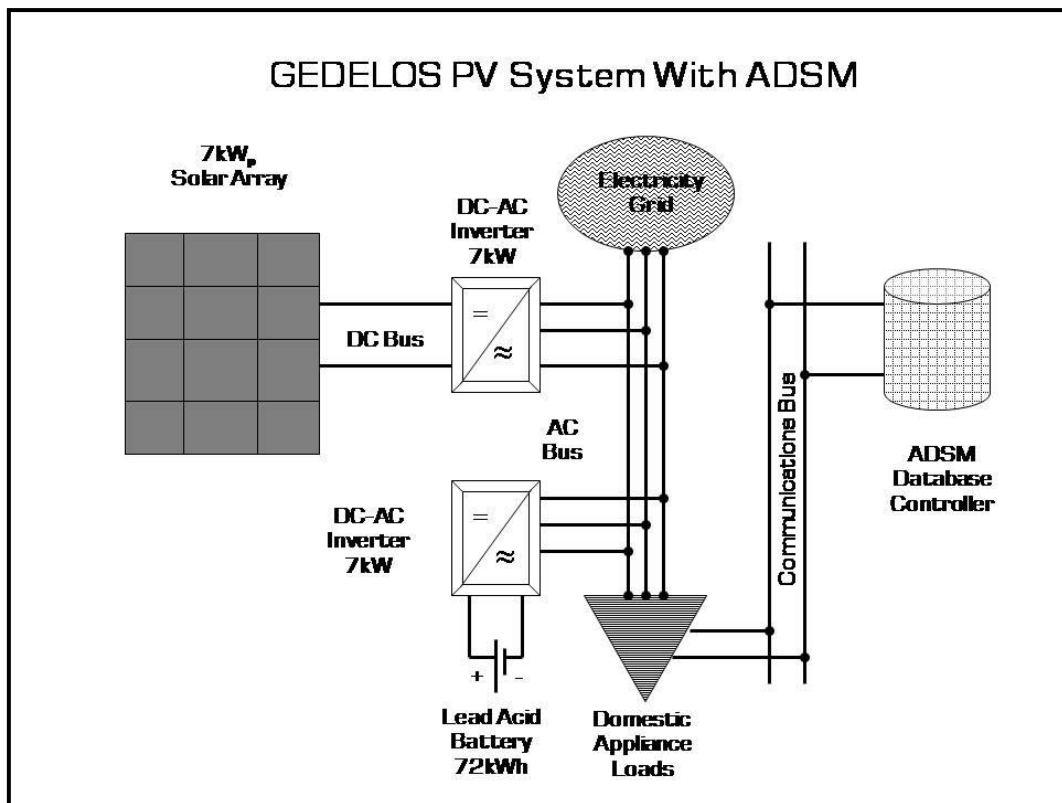


**Figure 7: Schematic Representation of the GEDELOS PV System**
**Source: Adopted from Self-Consumption of PV Electricity With Active Demand Side Management:**
**The GEDELOS-System [25]**

In this system, the load is served when there is sufficient solar power to do so. Thus, the temporal availability of solar power dictates when the load is served rather than the demand for power dictating when the solar power is needed.

Matching the load to the available power requires that the demand for energy from operating each appliance is known in advance [26]. This is achieved by capturing information about the power demand of each appliance into a database. An algorithm is then used to match the available solar power from the array and the battery with the combination of loads that minimises the amount of power that will be drawn from the grid [25]. The ADSM system ensures the optimal PVSC by selectively scheduling each load so that it is served with solar power and, only if it becomes necessary, power from the grid.
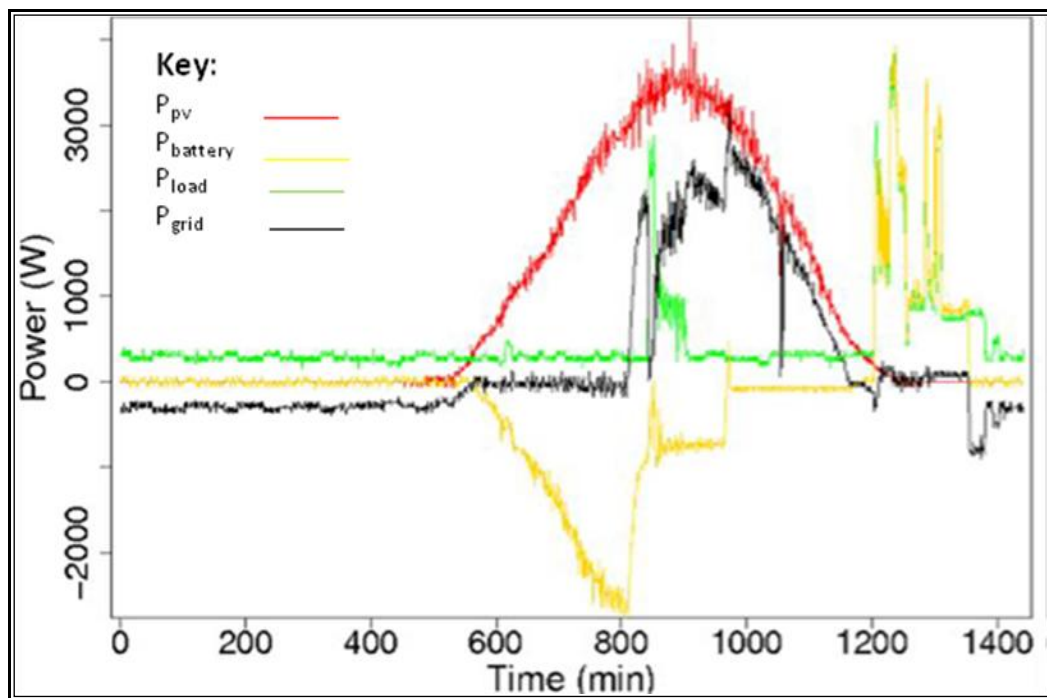


**Figure 8: Power Flows without ADSM (28/7/2010)**
**Source: Self-Consumption of PV Electricity With ADSM: The GEDELOS-System [25]**
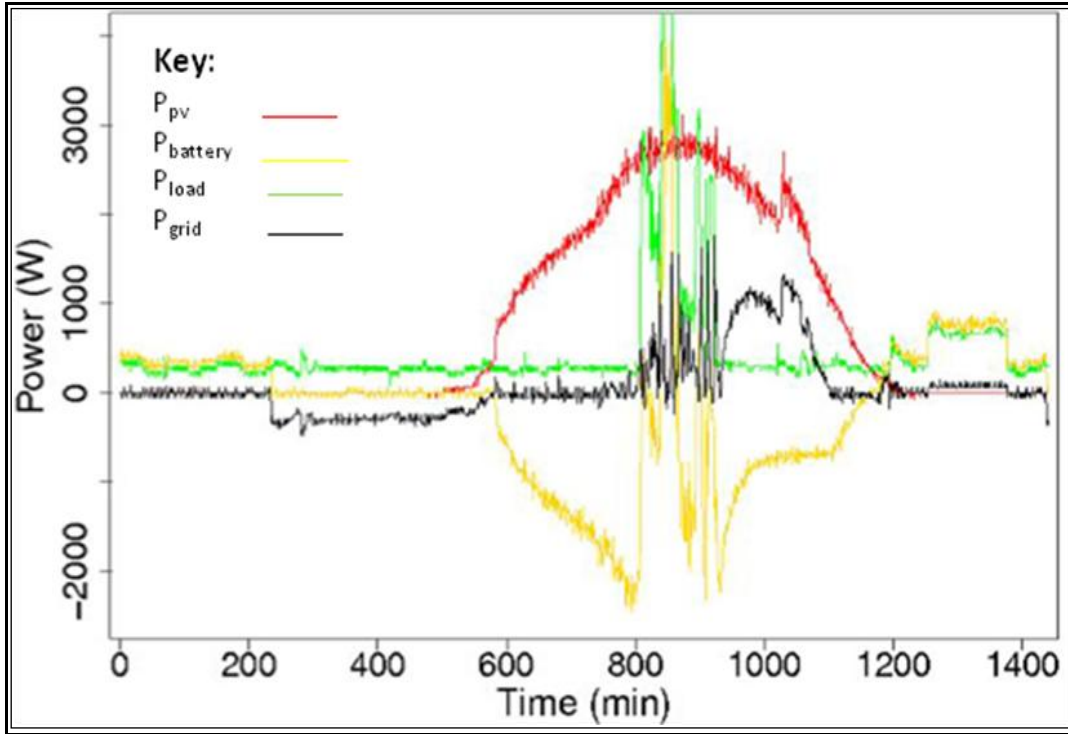
**Figure 9: Power Flows with ADSM (30/8/2010)**
**Source: Self-Consumption of PV Electricity With ADSM: The GEDELOS-System [25]**

Figure 8 and Figure 9 illustrates the power flows within the PVSC system with and without ADSM. In Figure 8, the demand for power is served immediately. During the day, this could involve importing electricity from the grid whilst during the evening temporal peaks in the load are served by power stored in the battery. During the evening, battery power is used as much as possible to power the load, even if this means importing electricity from the grid during the day. In Figure 9, where ADSM has been incorporated as part of the energy management system, the battery is randomly charged and discharged throughout the day so solar power can be supplied to the load. When the battery has completely discharged, it will be necessary to draw power from the grid to service the load. Making use of this idle capacity during the day still enables the load requirements in

the evening to be met by the battery. In this environment, the LaB can be deep-cycled to about 25% depth-of-discharge and charged to 95% of its rated capacity [25].

### 2.4.1 Measuring the PVSC Utilization

The approach taken to measure PVSC utilisation is based on the power flows within the system. This is illustrated in Figure 10, where the inputs to service the load originate from the solar array ($P_{pv}(t)$), the battery ($P_{bat}(t)$) or the grid ($P_{grid}(t)$).
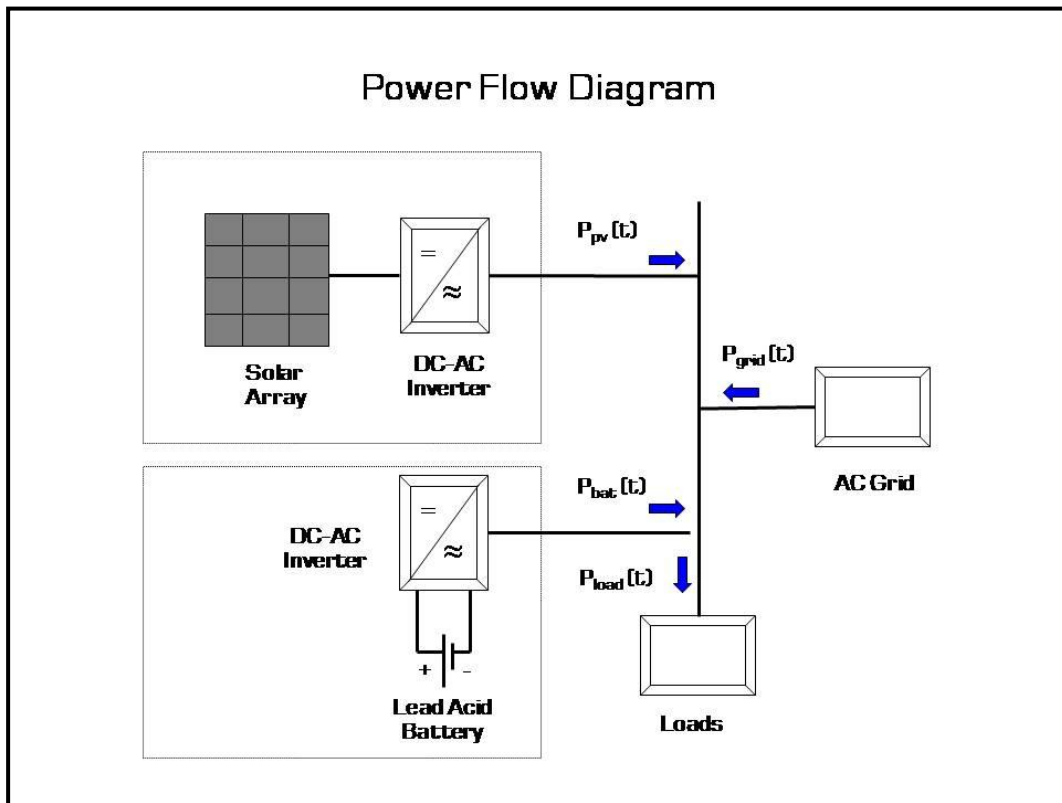


**Figure 10: Power Flows within the GEDELOS PV System**
**Source: Adopted from Self-Consumption of PV Electricity With ADSM: The GEDELOS-System [25]**

By inspection, the proportion of the solar ($P_{pv,\ load}(t)$) or battery ($P_{bat,load}(t)$) power flowing to the load is related by the PVSC factor $\varepsilon(t)$ [25]:

$$\varepsilon(t) \ = \ \frac{P_{pv,\ load}(t) + P_{bat,\ load}(t)}{P_{load}(t)} \tag{1}$$

Maximising the PVSC factor requires managing the load mix so that power for the load is derived from either the direct consumption of solar power or solar power stored in the battery system. The objective is to maximize the amount of solar power that is supplied to the load at the moment it is generated either by directing the solar power to supply the load or drawing upon the stored solar power in the battery system. In the GEDELOS PV system environment, by allowing the charging of the battery to have priority over the servicing of the load, the system allows solar power to be supplied to the load throughout the entire day.

In general, a higher $\varepsilon(t)$ is more desirable as this would mean that more solar and battery power is being used to serve the load. However, as the GEDELOS study suggests, increasing the ratio of the total battery capacity to the load will not necessarily increase the utilisation of solar energy in a PVSC system and that the PVSC factor saturates at 0.75 despite increasing the size of the battery system.

### 2.4.2 Summary

A defining feature of the GEDELOS study is that it introduces to the PVSC system ways to increase the amount of PVSC. Managing the load brings forth new possibilities in the way solar energy can be used to meet the changing demands for power. By scheduling

when the load draws power from the system to coincide with when the solar energy is available, more PVSC becomes possible.

Although LABs were used instead of LIBs, the study provides a method to measure the performance of each system within the PVSC system and the amount of power that they contribute towards PVSC. The PVSC factor can assist towards sizing the solar array and the battery storage system to maximize PVSC. As the PVSC system is connected to the grid, using a measure of the number of day's autonomy to size a battery bank may not be a sufficient measure to determine the size of the battery system that will maximize the amount of solar power used to supply the load. Indeed, in a high load situation, a low PVSC factor might mask that fact that PVSC is at a maximum and that energy efficiency measures need to be considered to ensure that the best use is made of the solar power available at that site.

# Chapter 3: Analytical Review of Lithium Ion Batteries

## 3.1    Background

Lithium ion batteries (LIB) were first commercialized in 1991 [27] and since then have been widely used in many applications from powering consumer electronic devices to providing energy for high power applications such as military equipment and electric vehicles [27].  LIBs are generally made into cylinders, buttons or prismatic geometries [28] with some LIBs being made as primary, non-rechargeable batteries whilst others possessing the ability to be recharged for re-use as secondary batteries [27, 28]. Commercially, they are popular because of their high energy density, lightweight and their tolerance to abusive operating conditions.

## 3.2    Electrochemical Changes in Lithium Ion Batteries

The charge-discharge process of LIBs essentially involves the transportation of lithium ions between anode and cathode.  As with other electrochemical batteries, the discharge potential is determined by the half reactions that take place at the anode and the cathode [29].  For the LIB battery, these half reactions are well documented in the literature [30] describing the intercalation and de-intercalation of lithium ions through the crystalline structure of the compounds that make up the host electrode.  Significantly, as the battery ages capacity loss and power fade begin to become apparent at both the anode and the cathode.  Whereas capacity loss results in the permanent loss of active material, power fade expresses itself in the reduction of the open circuit potential.

At the anode, capacity loss is primarily caused by the consumption of active material by the non-conducting solid electrolyte inter-phase (SEI) layer as well as the formation of cracks throughout the structure of the crystal from the repeated cycling of the battery [31, 32]. On the other hand, power fade is primarily caused by operating the battery at high temperatures and overcharging the battery or by discharging the battery beyond what it can tolerate [31]. As the battery ages, short-circuit currents flowing through strands of dendrites [33] become more probable and in the process, reducing the open circuit potential.

Alternately, for the cathode, charge capacity fading is a result of structural changes to the crystal that come about from over-cycling, chemical reaction and decomposition with the electrolytic material and the thickening [31] and degradation [34] of the SEI layer at the electrode [31]. The nature of the crystalline structure of the cathode also plays an important role in capacity fading in that high levels of intercalation and de-intercalation cause the crystal to expand and shrink resulting in the premature exfoliation of active material from the electrode [32, 35]. For this reason, lithium compounds that have crystal structures that can withstand the intercalation and de-intercalation forces arising from heavy cycling of the battery [36] tend to be used in commercial applications that involve high levels of power consumption.

## 3.3   Lithiated Iron Phosphate Cathodes

Lithiated iron phosphate (LFP) secondary batteries were first demonstrated in 1997 [37]. The discharge reaction taking place at the cathode can be represented by Equation 2:

$$\text{LiFePO}_4 - x\text{Li}^+ - x\text{e}^- \longrightarrow x\,\text{FePO}_4 + (1-x)\,\text{LiFePO}_4 \qquad (2)$$
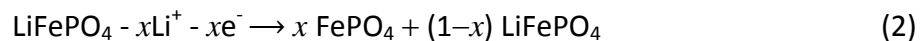
where $x$ represents the degree of lithiation at the cathode and the $FePO_4$ compound being what is retained upon delithiation of the LFP cathode [36-38]. A comparison of the electrochemical properties of the LFP battery and other cathode materials is shown in Table 2.

| Table 2: Chemical and Electrical Properties of Lithium Ion Batteries | | | | |
|---|---|---|---|---|
| **Property** | **Value** | | | |
| Cathode Material | $LiFePO_4$ | $LiMn_2O_4$ | $LiCoO_2$ | $Li_{1+x}Mn_{2-x}O_4$ |
| Anode Material | Graphite | Graphite | Graphite | $Ti_{5/3}O_4$ |
| Average Discharge Voltage (V) | 3.3 | 3.7 | 3.7 | 2.3 |
| Average Charge Voltage (V) | 4.0 | 3.9-4.5 | 3.9-4.2 | 3.9-4.5 |
| Specific Energy (Wh/kg) | 60-110 | 100-150 | 175-240 | 70 |
| Energy Density (Wh/L) | 125-250 | 125-250 | 400-640 | 120 |
| Specific Capacity (mAh/g) | 170 | 100-120 | 155 | 100-120 |
| Continuous Rate Capability (C) | 10-125 | >30 | 2-3 | 10 |
| Cycle Life at 100% D.O.D | 1000+ | 500+ | 500+ | 4000+ |
| Charge Temperature ($^0$C) | 0-45 | 0-45 | 0-45 | -20-45 |
| Discharge Temperature ($^0$C) | -30-60 | -30-60 | -20-60 | -30-60 |
| Self-Discharge Rate (%/month) | 2-10 | 2-10 | 2-10 | 2-10 |
| Calendar Life (yr) | >5 | >5 | >5 | >5 |
| Source: Lithium Ion Batteries [35, 39] | | | | |

LFP cathodes formed from nano-sized crystals exhibit higher levels of specific energy capacities. The smaller size associated with nano-sized particles reduce the diffusion lengths for lithium ions migrating to the surface from the centre of the crystal [40]. The shorter diffusion lengths and the increase in the number of crystals that agglomerate on the electrode increase the number of particles that can take part in a reaction and hence the electrochemical performance of the LFP battery [40, 41]. The electrochemical

performance of the nano-particles can further be enhanced by including carbon (about 5wt%) [42] which will allow a LFP battery to increase its specific energy capacity to its maximum theoretical level of 170mAhg$^{-1}$ [36] whilst still operating at stable open-circuit potentials.

Inside the LFP cathode, the lithium ions must first have sufficient energy (known as the activation energy) [43] before it can de-intercalate from the LiFePO$_4$ crystal into the electrolyte. As such, more capacity can be gained from operating the LFP cathode at higher temperatures [40, 44] but this is at the risk of a shorter life for the cathode [35].

### 3.3.1 Charge-Discharge Characteristics

The stability of the charge-discharge voltage is an important characteristic of the LFP battery. After a drop in its open-circuit potential from its first use, the LFP battery's open circuit discharge potential plateaus at 3.3-3.5V [40, 45, 46] with a corresponding charge voltage of approximately 4.0V [40]. The discharge curve of a commercial LFP battery is shown in Figure 11.
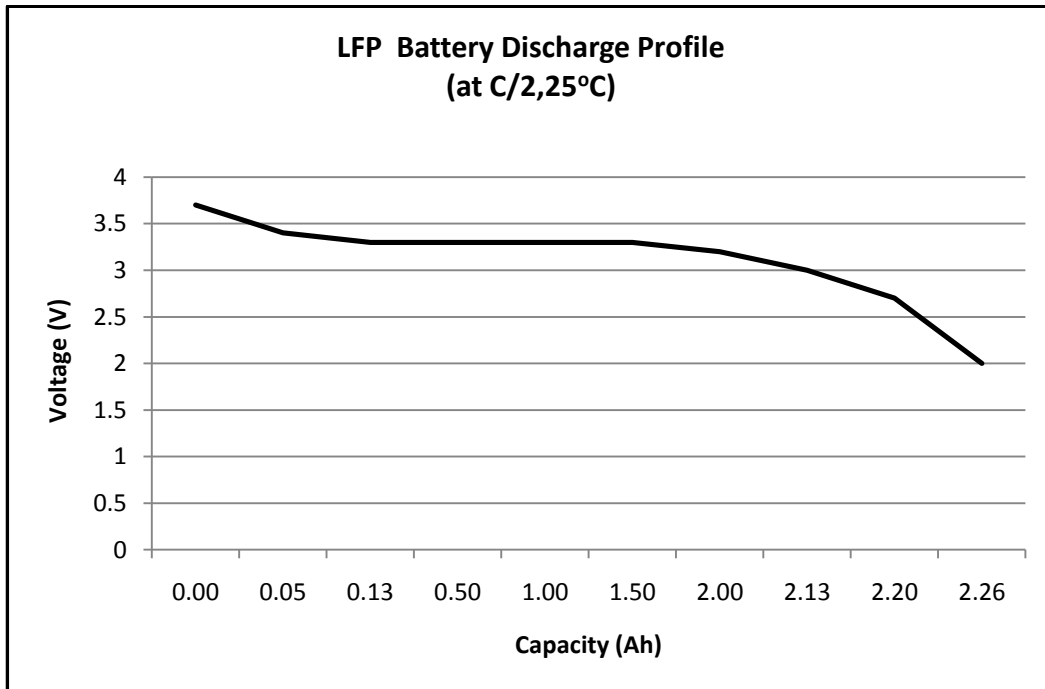
**Figure 11: A123-ANR26650-M1 Discharge Curve**
**Source: High Power Lithium Ion ANR26650-M1 [47]**

Between each charge and discharge cycle, it is possible to vary the discharge rates to maximize the battery capacity. Moreover, pulse charging the LFP battery can incrementally maximize the amount of charge provided to the battery [38]. Generally, the discharge profile of the LFP battery is stable with respect to changes in temperature with the exception when it operates in sub-zero temperatures, where the lower diffusivities reduce the battery capacity and the open circuit potential (~3.2V at temperatures $< -10^0$C) [48].

### 3.3.2 Loss Characteristics of the A123-ANR26650-M1

All LFP batteries exhibit loss with each charge-discharge cycle. The characteristic of this loss is determined by such factors as its crystal size, the molecular composition of the electrodes and the increased polarization and ohmic losses caused by the battery's aging

mechanisms [38, 49-51]. As such, these effects are made apparent by a drop in the battery's capacity and its output power.

Various experimental studies conducted under different environmental conditions have attempted to model the impact of the losses on the electrical output of the LFP battery [52, 53]. In regards to the A123-ANR26650-M1 nano-phosphate LFP cell, it has been posited that the loss can be estimated by Equation 3 [54]:

$$Q_{loss} = B \times \exp\left(\frac{-E_a}{8.314 \times T}\right) \times (\tilde{A}_h)^z \tag{3}$$

where $Q_{loss}$ is the percentage of capacity loss, B is the exponential pre-factor, $E_a$ is the activation energy ($Jmol^{-1}$), T is the absolute temperature (K), z is the power-law factor and $\tilde{A}_h$ is the power throughput as determined by the product of the battery capacity ($A_h$), depth-of-discharge (D.O.D) and the cycle number ($n_x$). Using this empirical model, it is then possible to numerically estimate the capacity loss of an A123-ANR26650-M1 cell during its lifecycle. As such the activation energy $E_a$ from Equation 3 is defined to be a constant at a particular C-rate such that [54]:

$$E_a = -370.3 \times C\text{-rate} + 31,700 \tag{4}$$

Thus, as the discharge rate increases, the capacity loss increases, lowering the overall power that can be obtained from the cell [35].

# Chapter 4: Simulation Methodology

## 4.1 Introduction

The simulations are performed using The Micropower Optimization Model (HOMER). HOMER (v2.68B) is a design tool that provides the ability to model a PVSC system using different combinations of system and cost inputs to generate power flows over a period of time [55].

The main phases that will be undertaken to conduct the simulation are shown in Table 3.

| Table 3: Phases of the Simulation | |
|---|---|
| **Phase** | **Simulation Methodology** |
| **1** | Define the Objectives |
| **2** | Detail the Scope |
| **3** | Determine the System Parameters |
| **Phase** | **Analytical Review of the Simulation** |
| **4** | Analyze and Discuss the Results |
| **Phase** | **Key Findings** |
| **5** | Document the Conclusions |
| **6** | Identify Recommendations |
| | |

## 4.2  Objective of the Simulation

The objective of the simulation is to model a PVSC system and to understand the power flows that occur within a PVSC environment. The primary focus is to simulate the operation of the second-life LFP battery in a PVSC system under conditions of primary loads that have to be served without delay and deferrable loads that can be served at a later time.

## 4.3  Simulation Scope

The simulation will examine PVSC for two residential properties located in Hydro-Quebec, Canada and Newcastle, United Kingdom [56]. Although HOMER is a cost-optimization program, the levelised cost and the payback period for each installation will not be examined in this simulation.

## 4.4  System Parameters Definition

The set-up for this simulation is illustrated in Figure 12 with the implementation of the system parameters documented in Appendix 1. The parameters of each system are chosen to reflect what would typically be used in residential solar systems. The capacity of the solar and the battery systems will be held constant in the simulations as increasing these capacities would likely increase the amount of PVSC. However, the simulation uses a solar array that is sized to reflect the average size of a residential solar system and the size of the battery reflects the largest possible size for safe operation in a residential environment.
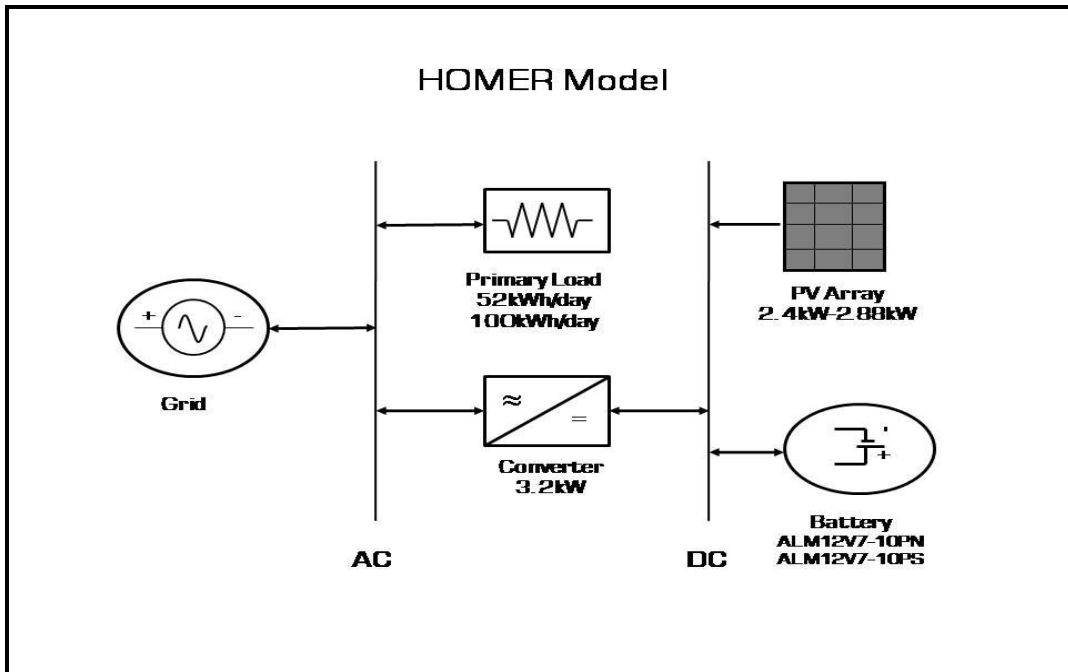
**Figure 12: HOMER Model**

## 4.4.1 Solar Profile

The average monthly solar radiation profiles of the two sites are shown in Figure 13 and Figure 14.
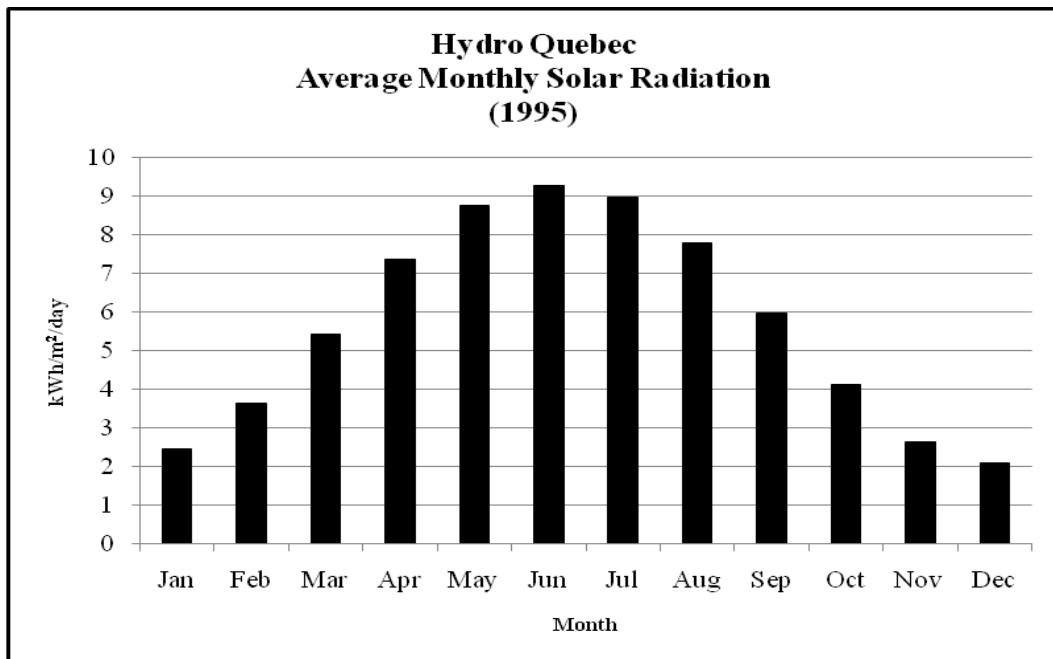


**Figure 13: Average Monthly Solar Radiation (Hydro Quebec, 1995)**

**Source: NASA Surface Meterology and Solar Energy [57]**
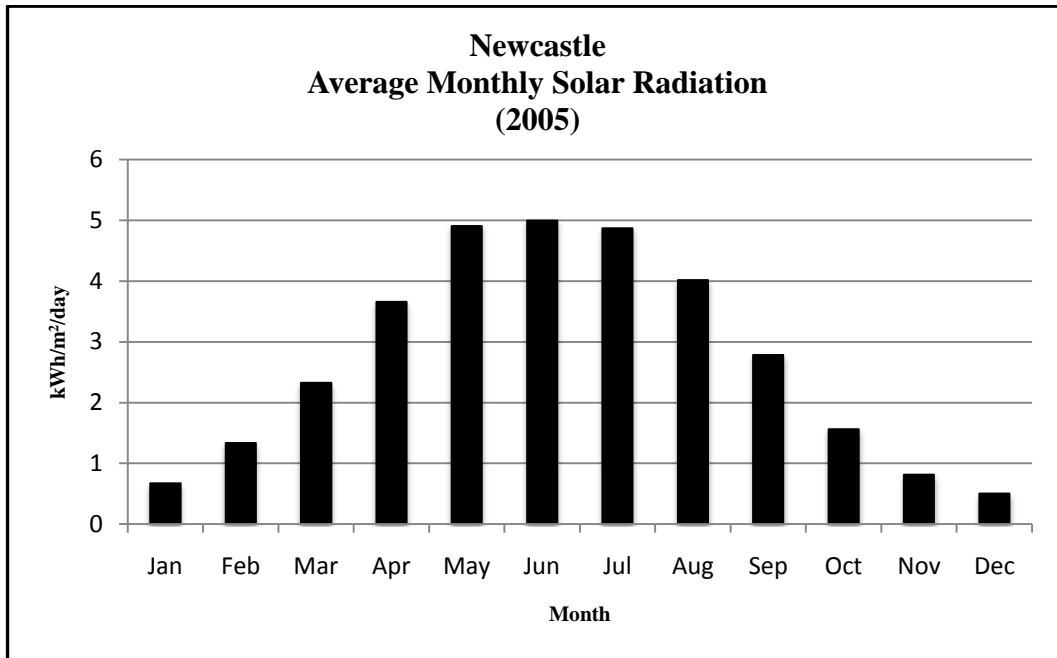
**Figure 14: Average Monthly Solar Radiation (Newcastle, 2005)**

**Source: NASA Surface Meterology and Solar Energy [57]**

In the model, each PVSC system has a roof-mounted solar array (2-3kWp) that mimics the average size of a solar array under European conditions [19, 58] with each panel rated at 240W.

### 4.4.2 Primary Load Profile

The daily average primary load profiles of the two residential properties [56] are shown in Figure 15 and Figure 16. These profiles reflect the actual, measured energy consumption patterns of a detached dwelling in Hydro-Quebec and a flat in Newcastle [56]. The occupants of the dwelling are not provided but a mother and two children occupied the flat [56].
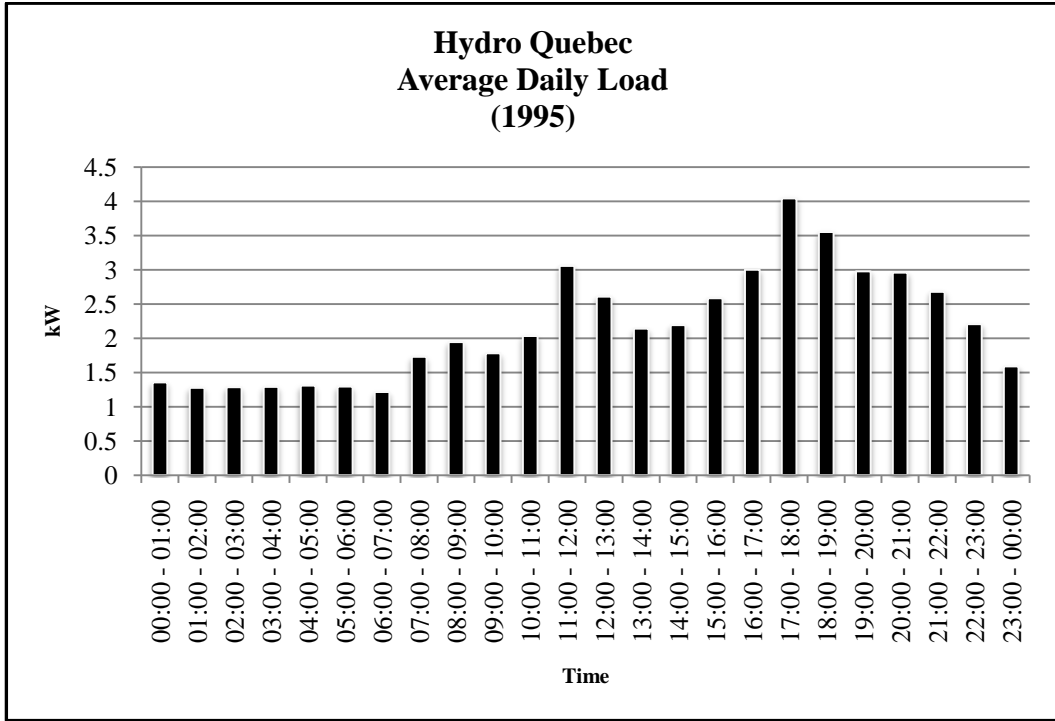
**Figure 15: Average Daily Load Profile (Hydro Quebec, 1995)**

**Source: The Simulation of Building Integrated Fuel Cell and Other Cogeneration Systems [56]**
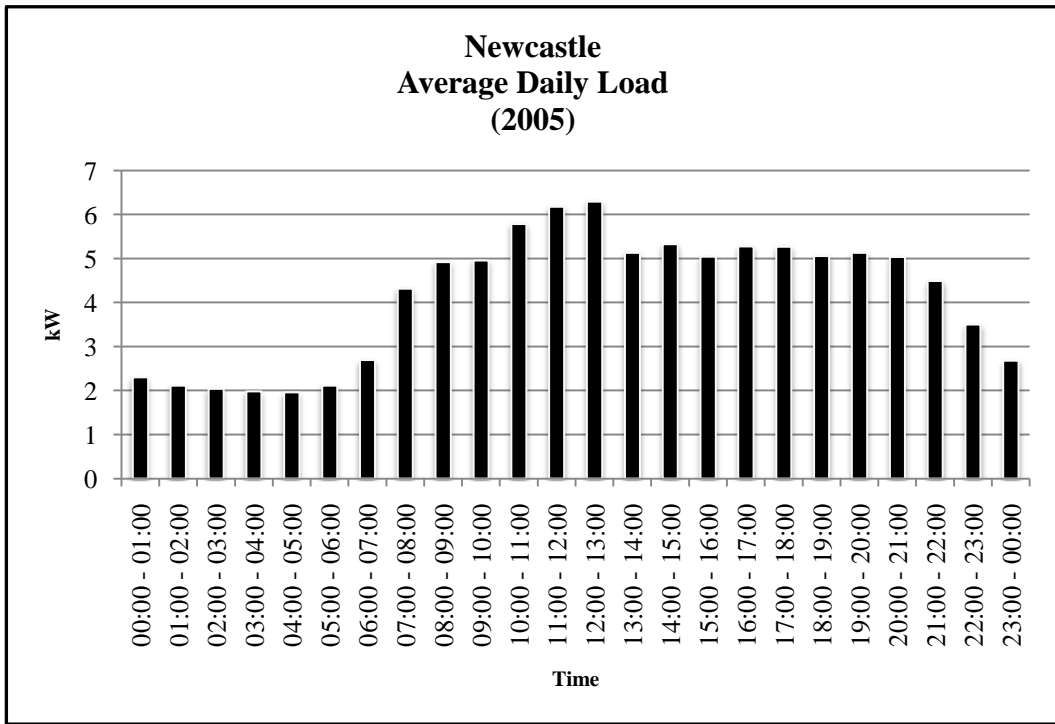


**Figure 16: Average Daily Load Profile (Newcastle, 2005)**

**Source: The Simulation of Building Integrated Fuel Cell and Other Cogeneration Systems [56]**

### 4.4.3 Deferrable Load Profile

The deferrable load is based on categorizing household appliances as cold, wet, lighting, brown or miscellaneous appliances [59, 60]. For the Newcastle site, those categorized as wet appliances (washing machines, tumble dryers etc) were considered as deferrable loads and subtracted from the primary load. To determine the deferrable load for the Canadian site, the total of the percentage of the hourly load attributed to the wet appliances (dishwashers, clothes-washers, clothes-dryers and distributed hot water heating) was first calculated and then subtracted from the primary load. The deferrable load profiles are shown in Figure 17 and Figure 18.
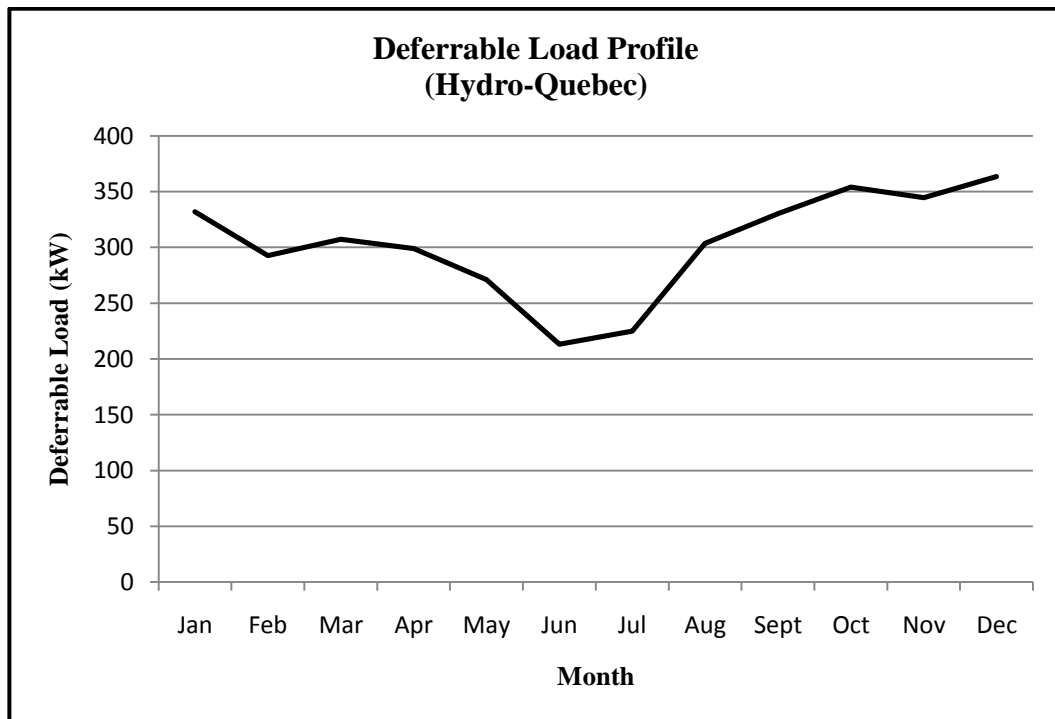


**Figure 17: Deferrable Load (Hydro-Quebec)**
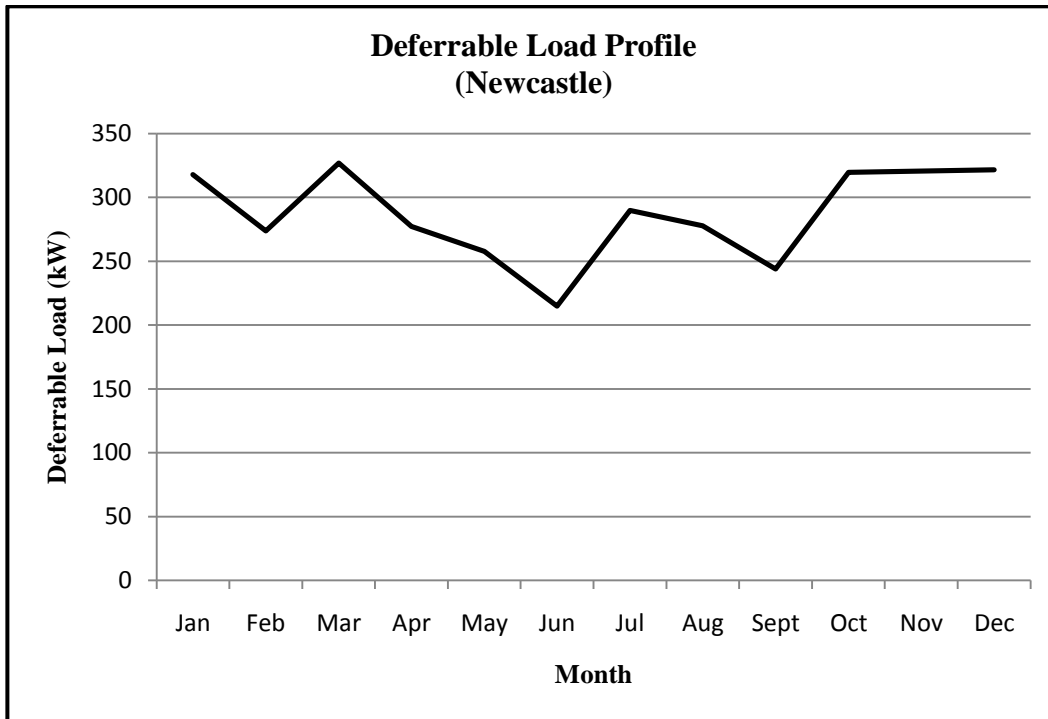
**Figure 18: Deferrable Load (Newcastle)**

HOMER uses a "storage tank" to determine when the deferrable load is served [55]. The tank size, initially defined by the user, sets the maximum amount of energy allocated for the deferrable load to be served. When the level of the tank falls to zero the load must be served by the available energy sources. To ensure the deferrable load is served at least once a week, the initial tank size is set to $1/52 \times$ the annual deferrable load.

### 4.4.4  Capacity Curve for ALM-12V7 Module

The LIB used in the simulation is based upon the A123 System ALM-12V7 lithium ion battery module. The capacity curve for a new ALM-12V7 module as illustrated in Figure 19 which is derived from the manufacturer's datasheets [61]. Each module is nominally rated at 4.6Ah at 13.2V [61]. A new battery in the model (called ALM12V7-10PN) consists of 10 strings connected in parallel, with each string containing 4 modules

connected in series. This is the maximum configuration possible [61] giving a battery with a nominally rated output of 46Ah at 52.8V.

**Capacity Curve For ALM-12V7 Module**

Figure showing capacity (Ah) versus discharge current (A):

| Discharge Current (A) | Capacity (Ah) |
|---|---|
| 23 | 48.5 |
| 46 | 46.9 |
| 92 | 46.2 |
| 184 | 45.8 |
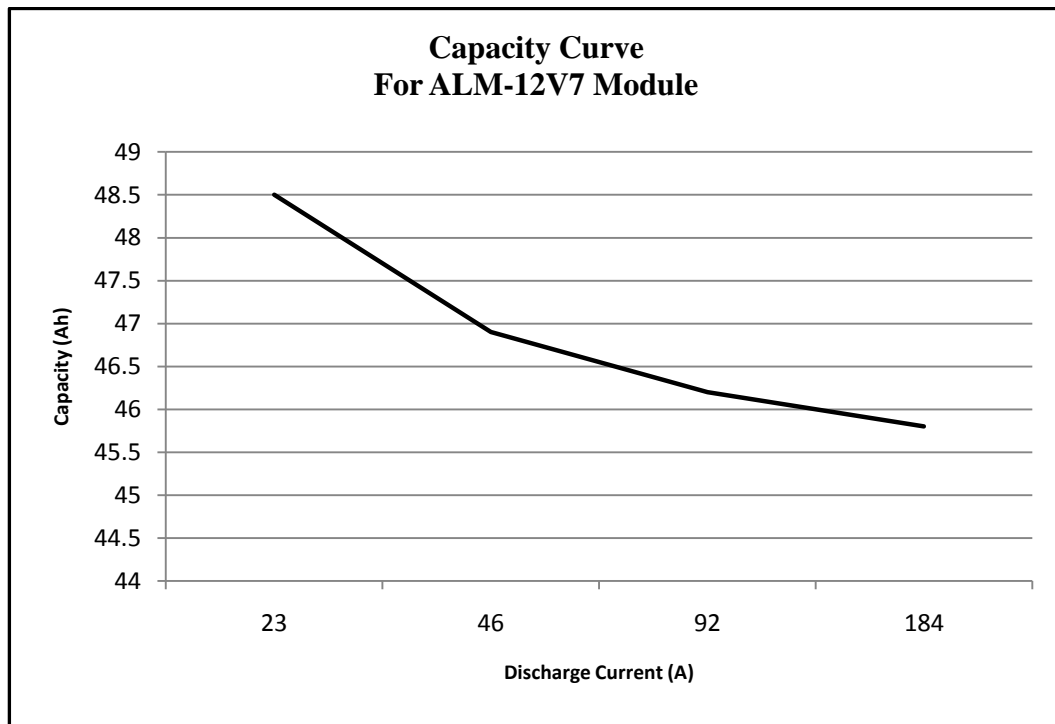
**Figure 19: Capacity Curve for the ALM-12V7 Module**
**Source: A123 ALM-12V7 User's Guide [61]**

A second-life LFP battery is assumed to have the same capacity characteristic as the new one. Capacity fade arising from persistent cycling is taken into account by assuming that the second-life battery (called ALM12V7-10PS) carries only 80% of the capacity of a new battery with a nominal capacity of 36.8Ah at 52.8V. Each battery has been modelled to retain a minimum state-of-charge of 20% as in the Sol-Ion Project [18].

### 4.4.5   Cycle Life Curve For ALM-12V7 Module

A numerical approach was used to calculate the cycle life curve.  Firstly, Equation 4 is used to evaluate $E_a$ ($E_a$ = 31, 329.700) at $C_1$ and T= 298K.  Secondly, Equation 3 can be re-arranged such that:

$$\text{Ln}\left(Q_{loss}\right) = \text{Ln}\left(B\right) + \left(\frac{-E_a}{8.314 \times T}\right) + z\,\text{Ln}\left(\tilde{A}_h\right) \tag{5}$$

Noting that $\tilde{A}_h = n_x$ (number of charge-discharge cycles) $\times$ D.O.D $\times$ battery capacity then this implies that for a fixed battery capacity, Ln ($Q_{loss}$) is linear function of $n_x$ and the D.O.D.  Using the manufacturer's datasheet for a new A123-ALM12V7 [61], the $Q_{loss}$ after each charge-discharge cycle was measured and substituted into Equation 5, noting that this is specific to a particular D.O.D (in this case D.O.D = 100%).  These results are shown in Table 4.

| Table 4: Loss Characteristics of ALM12V7 Module | | | | | | |
|---|---|---|---|---|---|---|
| $Q_{loss}$ | $n_x$ | $A_h$ | D.O.D | $\tilde{A}_h$ | $Ln(\tilde{A}_h)$ | $Ln(Q_{loss})$ |
| 0.02143 | 500 | 4.6 | 1 | 2,300 | 3.36172 | -1.66898 |
| 0.03920 | 1000 | 4.6 | 1 | 4,600 | 3.6627 | -1.40679 |
| 0.06071 | 1500 | 4.6 | 1 | 6,900 | 3.83884 | -1.21673 |
| 0.08214 | 2000 | 4.6 | 1 | 9,200 | 3.96378 | -1.08544 |
| 0.09643 | 2500 | 4.6 | 1 | 11,500 | 4.06069 | -1.01578 |
| 0.11429 | 3000 | 4.6 | 1 | 13,800 | 4.13988 | -0.94199 |
| 0.12143 | 3500 | 4.6 | 1 | 16,100 | 4.20682 | -0.91567 |
| 0.13571 | 4000 | 4.6 | 1 | 18,400 | 4.2648 | -0.86738 |
| 0.14286 | 4500 | 4.6 | 1 | 20,700 | 4.31597 | -0.84508 |
| 0.15714 | 5000 | 4.6 | 1 | 23,000 | 4.36172 | -0.80371 |
| 0.16786 | 5500 | 4.6 | 1 | 25,300 | 4.4031 | -0.77505 |
| 0.17500 | 6000 | 4.6 | 1 | 27,600 | 4.44091 | -0.75696 |
| 0.18214 | 6500 | 4.6 | 1 | 29,900 | 4.47567 | -0.73959 |
| 0.19286 | 7000 | 4.6 | 1 | 32,200 | 4.50786 | -0.71475 |
| Source: A123 System's Manufacturer's Specifications [61] | | | | | | |

Linear regression is then used to determine the pre-exponential factor (B) and the power law factor (z) at the $C_1$ rate [54]. From the regression analysis, z = 0.8257, and upon solving, B = 3,797.0587 at the $C_1$ rate and 298K. As shown in Table 5, the $R^2$ factor was 0.9892.

## Table 5: Summary Output of Regression Analysis

**Regression Statistics**

| | |
|---|---|
| Multiple R | 0.9946 |
| R Square | 0.9892 |
| Adjusted R Square | 0.9883 |
| Standard Error | 0.0301 |
| Observations | 14 |

**ANOVA**

| | df | SS | MS | F | Significance F |
|---|---|---|---|---|---|
| Regression | 1 | 1.0017 | 1.0017 | 1102.9213 | 3.52E-13 |
| Residual | 12 | 0.0109 | 0.0009 | | |
| **Total** | **13** | **1.0126** | | | |

| | Coefficients | Standard Error | t Stat | P-value | Lower 95% | Upper 95% | Lower 95.0% | Upper 95.0% |
|---|---|---|---|---|---|---|---|---|
| Intercept | -4.4033 | 0.1033 | -42.6175 | 0.0000 | -4.6285 | -4.1782 | -4.6285 | -4.1782 |
| Ln(Ãh) | 0.8257 | 0.0249 | 33.2103 | 0.0000 | 0.7715 | 0.8798 | 0.7715 | 0.8798 |

After substituting into Equation 3, and noting that at the end of the battery's life, $Q_{loss} = 1$ and using MS Excel's solver function, it is then possible to find the maximum number of charge-discharge cycles ($n_x$) such that at various D.O.D, $Q_{loss} = 1$. The process is then repeated for $Q_{loss} = 0.2$ for the battery. The number of cycles at each D.O.D is then subtracted from the maximum number of charge-discharge cycles to give the remaining number of charge-discharge cycles for a second-life battery. These results are shown in Table 6 and Table 7 with the cycle life curves illustrated in Figure 20.
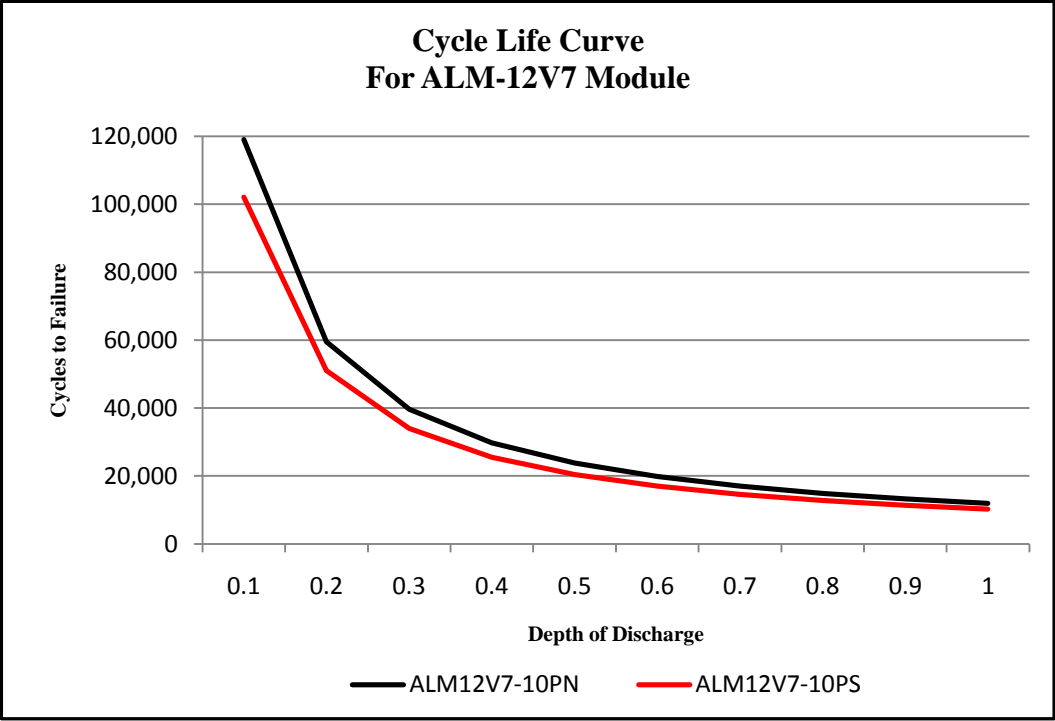
**Figure 20: Cycle Life Curve for the ALM-12V7 Module**

## Table 6: Cycle Life Calculations for ALM 12V7 Battery

| B | $E_a$ | R | T | z | $A_h$ | Cycle No | D.O.D | $\tilde{A}_h$ | $Q_{loss}$ | $A_h \times (1 - Q_{loss})$ |
|---|---|---|---|---|---|---|---|---|---|---|
| 3,797 | 31,330 | 8.314 | 298 | 0.82567 | 4.6 | 11,902 | 1 | 54,748 | 1.0000 | 0.0000 |
| 3,797 | 31,330 | 8.314 | 298 | 0.82567 | 4.6 | 13,224 | 0.9 | 54,748 | 1.0000 | 0.0000 |
| 3,797 | 31,330 | 8.314 | 298 | 0.82567 | 4.6 | 14,877 | 0.8 | 54,748 | 1.0000 | 0.0000 |
| 3,797 | 31,330 | 8.314 | 298 | 0.82567 | 4.6 | 17,002 | 0.7 | 54,748 | 1.0000 | 0.0000 |
| 3,797 | 31,330 | 8.314 | 298 | 0.82567 | 4.6 | 19,836 | 0.6 | 54,748 | 1.0000 | 0.0000 |
| 3,797 | 31,330 | 8.314 | 298 | 0.82567 | 4.6 | 23,803 | 0.5 | 54,748 | 1.0000 | 0.0000 |
| 3,797 | 31,330 | 8.314 | 298 | 0.82567 | 4.6 | 29,754 | 0.4 | 54,748 | 1.0000 | 0.0000 |
| 3,797 | 31,330 | 8.314 | 298 | 0.82567 | 4.6 | 39,672 | 0.3 | 54,748 | 1.0000 | 0.0000 |
| 3,797 | 31,330 | 8.314 | 298 | 0.82567 | 4.6 | 59,509 | 0.2 | 54,748 | 1.0000 | 0.0000 |
| 3,797 | 31,330 | 8.314 | 298 | 0.82567 | 4.6 | 119,017 | 0.1 | 54,748 | 1.0000 | 0.0000 |

## Table 7: Cycle Life Calculations for ALM 12V7 Battery (20% Loss)

| B | $E_a$ | R | T | z | $A_h$ | Cycle No | D.O.D | $\tilde{A}_h$ | $Q_{loss}$ | $A_h \times (1 - Q_{loss})$ |
|---|---|---|---|---|---|---|---|---|---|---|
| 3,797 | 31,330 | 8.314 | 298 | 0.82567 | 4.6 | 1,695 | 1 | 7,795 | 0.2000 | 3.6800 |
| 3,797 | 31,330 | 8.314 | 298 | 0.82567 | 4.6 | 1,883 | 0.9 | 7,795 | 0.2000 | 3.6800 |
| 3,797 | 31,330 | 8.314 | 298 | 0.82567 | 4.6 | 2,118 | 0.8 | 7,795 | 0.2000 | 3.6800 |
| 3,797 | 31,330 | 8.314 | 298 | 0.82567 | 4.6 | 2,421 | 0.7 | 7,795 | 0.2000 | 3.6800 |
| 3,797 | 31,330 | 8.314 | 298 | 0.82567 | 4.6 | 2,824 | 0.6 | 7,795 | 0.2000 | 3.6800 |
| 3,797 | 31,330 | 8.314 | 298 | 0.82567 | 4.6 | 3,389 | 0.5 | 7,795 | 0.2000 | 3.6800 |
| 3,797 | 31,330 | 8.314 | 298 | 0.82567 | 4.6 | 4,236 | 0.4 | 7,795 | 0.2000 | 3.6800 |
| 3,797 | 31,330 | 8.314 | 298 | 0.82567 | 4.6 | 5,649 | 0.3 | 7,795 | 0.2000 | 3.6800 |
| 3,797 | 31,330 | 8.314 | 298 | 0.82567 | 4.6 | 8,473 | 0.2 | 7,795 | 0.2000 | 3.6800 |
| 3,797 | 31,330 | 8.314 | 298 | 0.82567 | 4.6 | 16,946 | 0.1 | 7,795 | 0.2000 | 3.6800 |

To validate our calculations, $Q_{loss(A123)}$ from the manufacturer's specifications is compared to $Q_{loss(model)}$ in Figure 21. The results show that the battery used in the model experiences more loss with each cycle than the one estimated by the manufacturer. Noting that the manufacturer's datasheets only provides details up to 7,000 cycles, this is likely to mean that the PVSC factor derived from the simulation will be much smaller than it would be in a live environment.
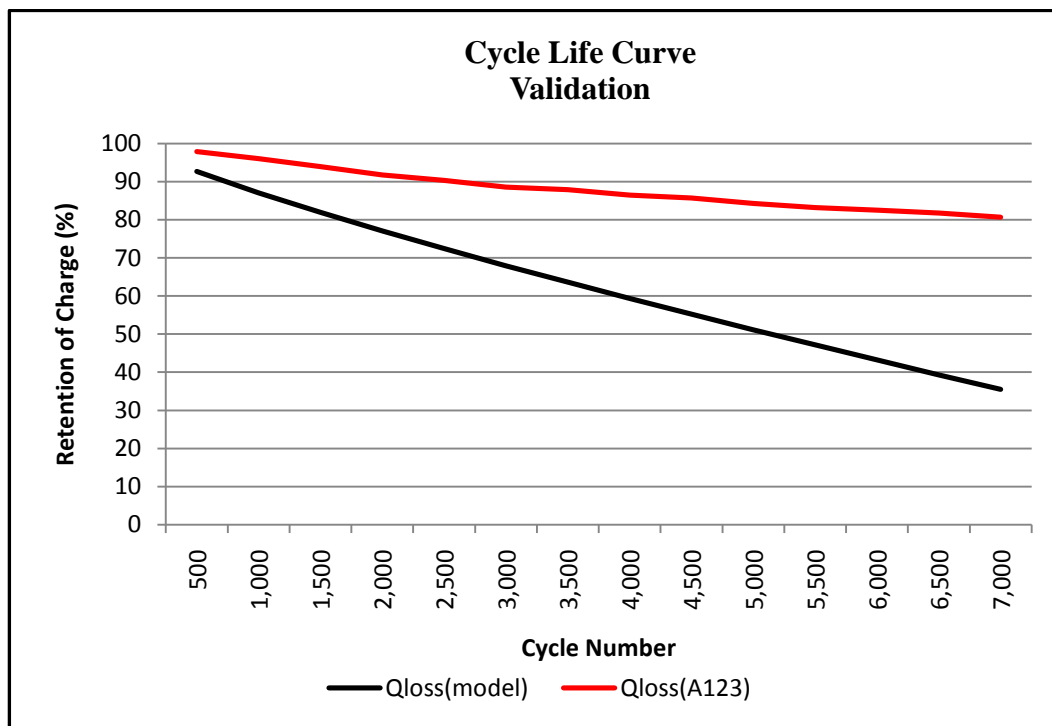


**Figure 21: Battery Loss Characteristic Validation**

### 4.4.6 Calculation of PVSC Factors

HOMER generates data on the energy flows with its internal algorithms. The total solar and battery power used to serve the load is the output of the inverter less any grid sales. Calculating the amount of PVSC using this method allows any inverter losses to be excluded from the amount of PVSC.

### 4.4.7 Cost Parameters

Table 8 provides details of the costs used in the simulation. The costs do not include conversion costs to a second-life battery.

| Table 8: System Component Costs | | | | |
|---|---|---|---|---|
| **Hydro Quebec, Canada** | | | | |
| Latitude | 45$^o$46'N | [62] | | |
| Longitude | 71$^o$41'W | [62] | | |
| Interest Rate (Bank of Canada) (%) | 11.25 | [63] | | |
| Annual Inflation Rate (%) | 1.93 | [64] | | |
| Real Interest Rate (%) | 9.32 | [Calculated] | | |
| | | | | |
| **Newcastle On The Tyne, UK** | | | | |
| Latitude | 54$^o$58'N | [62] | | |
| Longitude | 1$^o$36'W | [62] | | |
| Interest Rate (Clysdale Bank) (%) | 6.00 | [65] | | |
| Annual Inflation Rate (%) | 3.47 | [64] | | |
| Real Inflation Rate (%) | 2.53 | [Calculated] | | |
| | | | | |
| **Costs Normalized to $USD** | | | | |
| **Solar Panel** | **Cost (£)** | **Exchange Rate [66]** | **(USD)** | |
| HIT-N240SE10 - 240w Sanyo Framed | 640.00 | £:USD -> 1:1.5903 | 1,017.60 | [67] |
| **Converter** | **Cost (AUD)** | **Exchange Rate [66]** | **(USD)** | |
| SMA Sunny Boy 3000W Grid | 4,000.00 | AUD:USD -> 1:1.036 | 4,144.00 | [68] |
| | | | | |
| **LiFePO4 Battery Module** | **Cost (€)** | **Exchange Rate [66]** | **(USD)** | |
| A123 ALM12V7 (10P-N) | 1,799.00 | €: USD -> 1:1.3309 | 2,394.29 | [69] |
| A123 ALM12V7 (10P-S) | 1,439.20 | €:USD -> 1:1.3309 | 1,915.43 | [69] |
| | | | | |
| **Electricity Tariffs** | **Cost ($C/kWh)** | **Exchange Rate [66]** | **(USD)** | |
| Base Plan Rate (Hydro Quebec) | 0.532 | $C:USD -> 1:1.00107 | 0.536 | [70] |
| Feed-In-Tariff Rate | 0.532 | $C:USD -> 1:1.00107 | 0.536 | [70] |
| Base Plan Rate (UK Power Co.) | 0.24 | £:USD -> 1:1.3309 | 0.315 | [71] |
| Feed-In-Tariff Rate | 0.43 | £:USD -> 1:1.3309 | 0.576 | [72] |

# Chapter 5: Review and Discussion of Simulation Results

## 5.1    PVSC Modelling

It was possible to simulate the sequence of energy flows of a PVSC system using the HOMER model.   At both the Newcastle and Canadian residential sites PVSC could be observed using the second-life battery model.
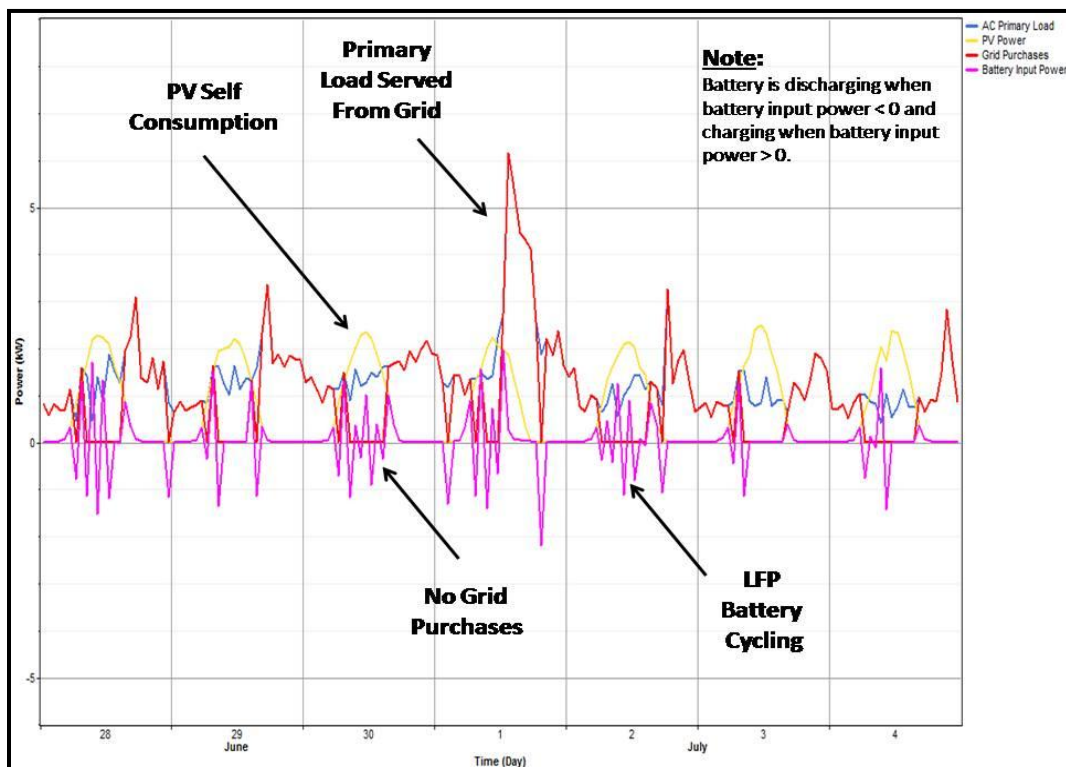


**Figure 22: PVSC (Second-Life Battery) Under Primary Load (Hydro Quebec)**
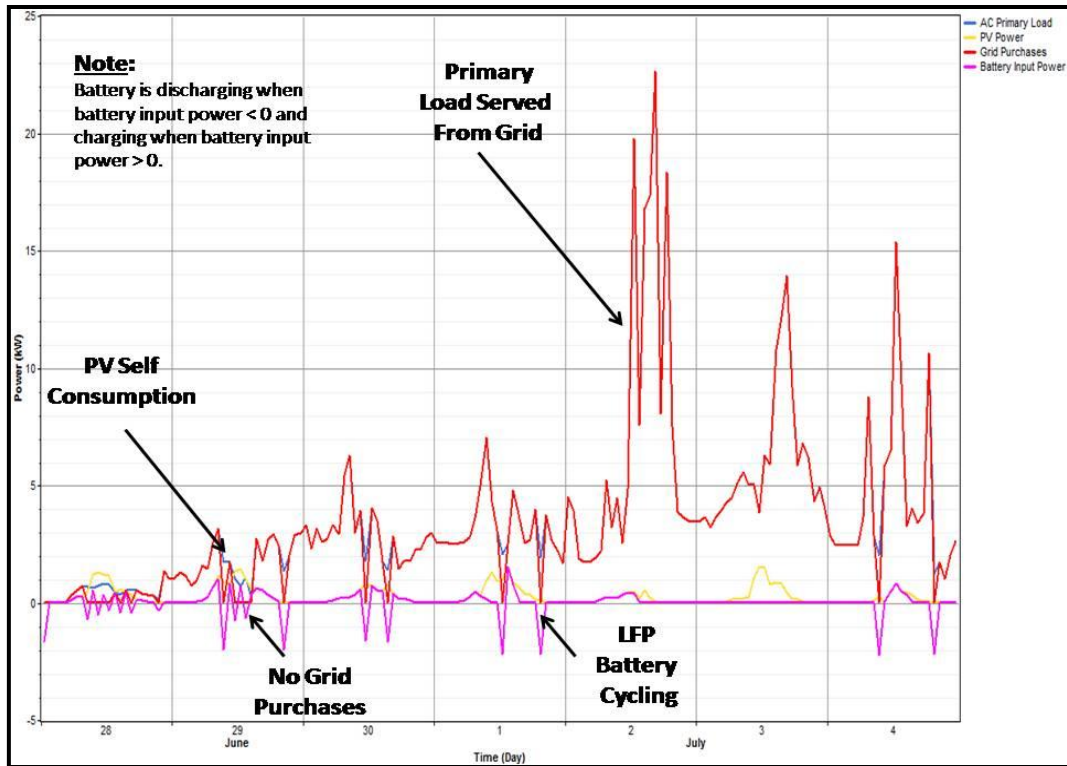
**Figure 23: PVSC (Second-Life Battery) Under Primary Load (Newcastle)**

As illustrated in Figure 22 and Figure 23, PVSC could be observed when there are no grid

purchases and only the solar power and the input from the battery is used to serve the load.

Moreover, it can be seen that under these circumstances there is frequent cycling of the

battery as power continuously flows from the PV panels to the battery and battery to the

load.

Also, according to the results in Table 9, at the Hydro-Quebec site, the amount of energy

throughput of the second-life battery is more than that of the new battery. As the round-

trip efficiency is the same for both batteries then there must be more input energy going

into the second-life battery than the new one even though the amount of available solar

energy is the same. The reason why this occurs is because the new battery has a smaller

maximum charge rate (2.1739 A/Ah) than the second-life battery (2.7171 A/Ah).  This

condition is a direct consequence of the limitations of the configuration of the battery.

| Table 9: Comparison of Battery Output Metrics | | | | |
|---|---|---|---|---|
| **Site** | **Battery** | **Energy Throughput (kWh/year)** | **Maximum Charge Rate (A/Ah)** | **Energy Loss (kWh/year)** |
| Hydro-Quebec | ALM12V7-10PN | 1,802 | 2.1739 | 188 |
| Hydro-Quebec | ALM12V7-10PS | 1,862 | 2.7171 | 194 |
| Newcastle | ALM12V7-10PN | 991 | 2.1739 | 102 |
| Newcastle | ALM12V7-10PS | 990 | 2.7171 | 102 |
| Source: Battery Output Data [Appendix 2] | | | | |

When there is available energy, HOMER limits the rate of power transfer to the battery

based on the maximum charge rate [55].  Thus, for the same amount of solar energy that is

available, less power will be supplied to the new battery than the second-life one.  By way

of contrast, at the Newcastle site, the energy throughput for both types of batteries are the

same and the lower levels of incident solar radiation means that the same amount of solar

power is passed through to the batteries.

In practice, large charge currents can damage a LIB such as that of a LFP battery.  The

fluctuating output from a solar panel can result in both undercharging and overcharging of

the battery.  This makes a buck-boost converter an integral component in the PVSC

circuitry.  Moreover, LIBs that can withstand large fluctuations in input current would

possibly be better suited to be used in a PVSC system than those that can only withstand

small charge currents.  As indicated in Chapter 3.0, this can limit the range of LIBs that

can be used in PVSC systems and that it may be necessary to that a solar panel's short circuit current is less than the maximum charge current of the battery. Also, it is important to note that the losses measured in Table 9 represent the predefined battery loss in the model and would take into account the capacity fade of the battery due to the battery's own internal loss mechanisms.

## 5.2 Deferrable Load Models

Simulations were performed to understand the behaviour of PVSC systems with deferrable loads. An example of a PVSC system that comprises of deferrable loads would be one where active demand side management is present to manage the loads.

As illustrated in Figure 24, the deferrable load profile is not necessarily served at the same time as the primary load. Where the deferrable load cannot be served by solar or battery power, HOMER will allocate power from the grid to ensure that the load is periodically served.
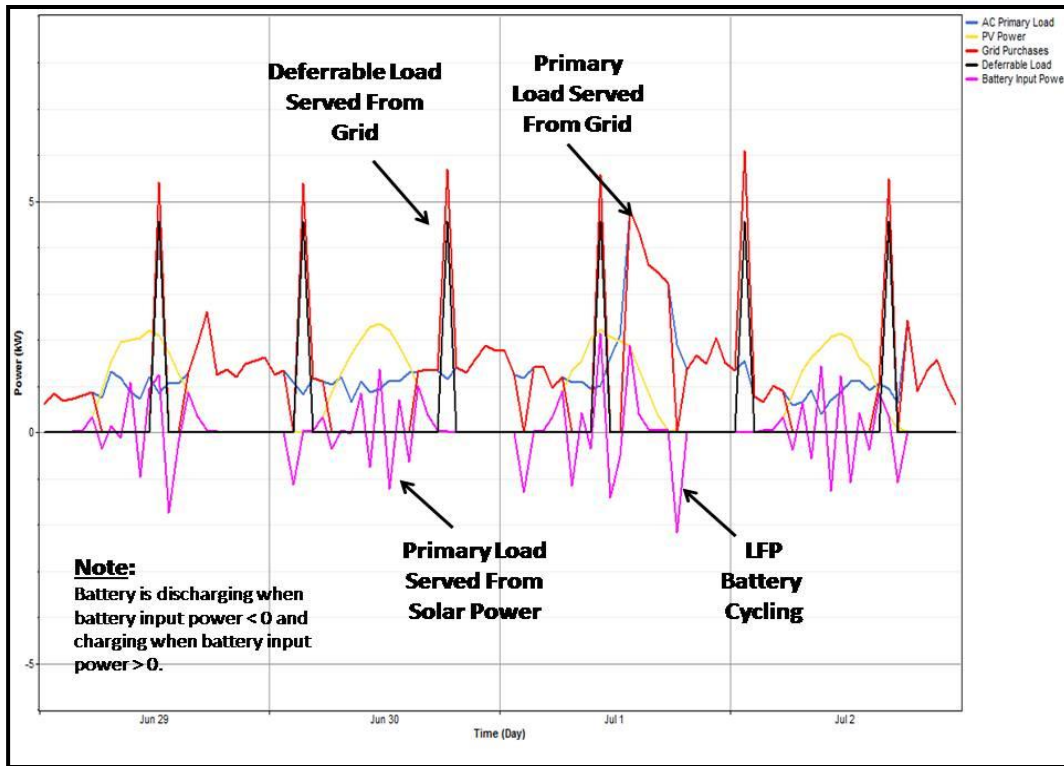
**Figure 24: Deferrable Load Response with Second-Life Battery (Hydro-Quebec)**

According to the simulations that were performed, it was not possible to service the deferrable load with solar and battery power by reducing the minimum state-of-charge and the deferrable load (by 10%). As illustrated in Figure 25, the deferrable load could be served through PVSC if it was reduced by 90% of its original value.
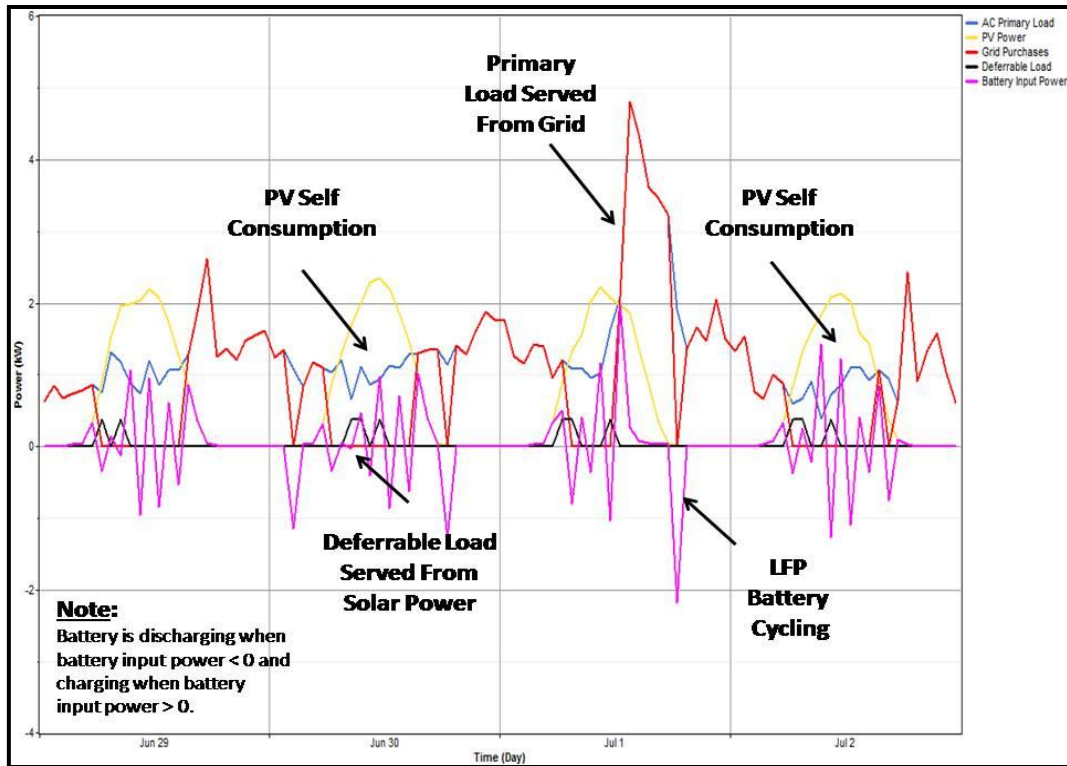
**Figure 25: Reduced Deferrable Load with Second-Life Battery (Hydro-Quebec)**

When the deferrable was reduced, the solar and battery power was being dispatched by HOMER to service both the primary and deferrable loads without any grid purchases of electricity. Thus, the amount of PVSC is limited by the demand for power and when increasing the size of the solar and battery system is not feasible, managing energy demand will become an important aspect in reducing the amount of grid supplied energy.

## 5.3 Battery State-of-Charge

Changes in the state-of-charge (SOC) for each battery are illustrated in Figure 26 and Figure 27. HOMER uses a kinetic model for the operation of the batteries [61] and cycles the batteries to their maximum depth-of-discharge whenever there is sufficient power in the battery to serve the load. The higher proportion of times the SOC of the new and second-life battery at Newcastle remained at 100% would suggest that there was insufficient solar and battery power to meet the high level of primary loads.
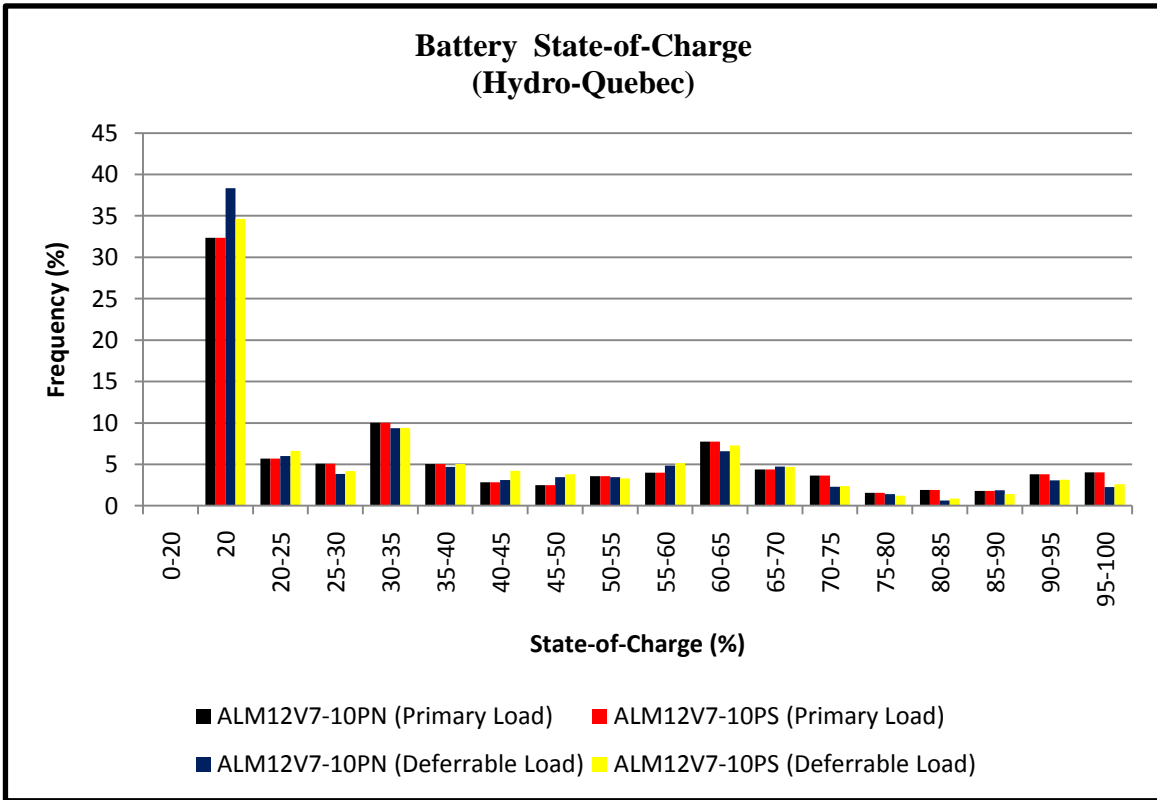


**Figure 26: Battery State-of-Charge (Hydro-Quebec)**

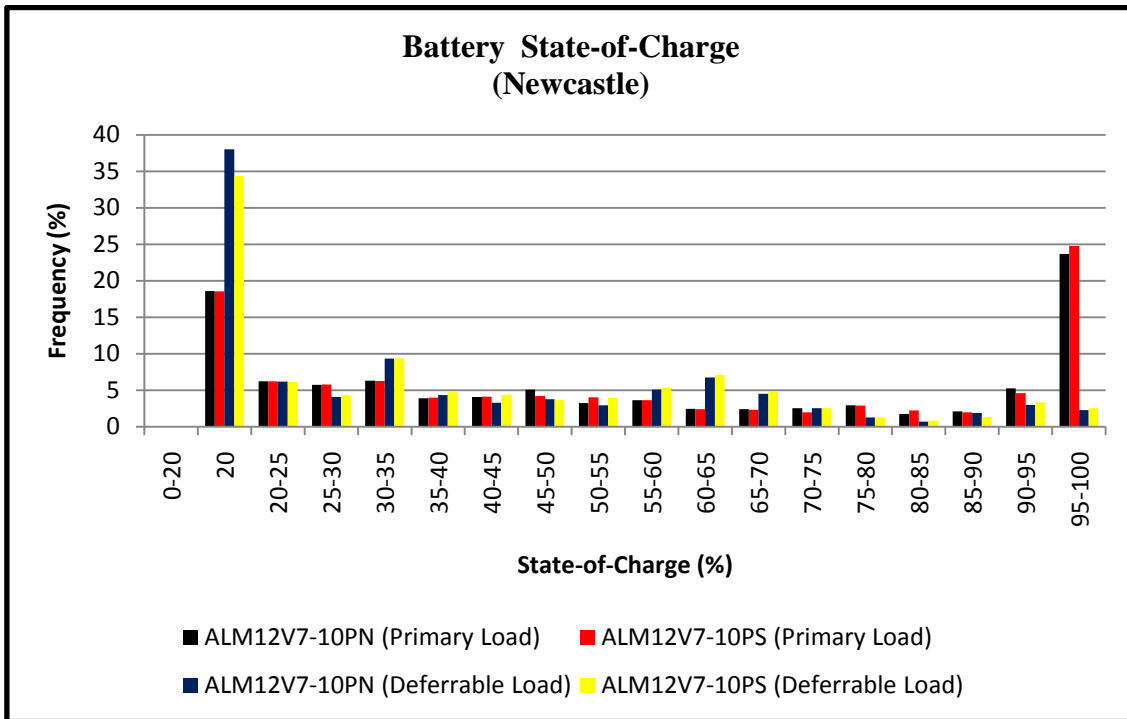**Figure 27: Battery State-of-Charge (Newcastle)**

By way of contrast, under deferrable load conditions, the higher frequency of times the batteries at both sites cycled to their maximum D.O.D would suggest that there is a much higher utilization of stored solar power when the loads are actively managed than when they are not. These results are consistent to the results from the GEDELOS PVSC environment [25].

## 5.4 PVSC Factor Calculations

The PVSC factor measures the extent of the load that is serviced by solar or battery power. From our calculations, it was found that the PVSC factor throughout the period of the simulation was quite low. The variation of the average monthly PVSC factors for Hydro-Quebec and Newcastle is collated in Table 10 and illustrated in Figure 28 and Figure 29.

| | Table 10: PVSC Factor Calculations | | | | | | | |
|---|---|---|---|---|---|---|---|---|
| | **Hydro-Quebec** | | | | **Newcastle** | | | |
| **Month** | $\varepsilon(t)$ ALM12V7-10PN | $\varepsilon(t)$ ALM12V7-10PS | $\varepsilon(t)$ def-load | **Primary Load (kW)** | $\varepsilon(t)$ ALM12V7-10PN | $\varepsilon(t)$ ALM1V7-10PS | $\varepsilon(t)$ def-load | **Primary Load (kW)** |
| Jan | 0.1679 | 0.1727 | 0.1888 | 1,693 | 0.0165 | 0.0165 | 0.0179 | 3,305 |
| Feb | 0.2020 | 0.2053 | 0.2241 | 1,488 | 0.0298 | 0.0298 | 0.0282 | 2,834 |
| Mar | 0.2417 | 0.2417 | 0.2554 | 1,580 | 0.0258 | 0.0258 | 0.0243 | 3,378 |
| Apr | 0.2388 | 0.2413 | 0.2521 | 1,574 | 0.0359 | 0.0359 | 0.0374 | 2,944 |
| May | 0.2508 | 0.2533 | 0.2698 | 1,423 | 0.0501 | 0.0501 | 0.0485 | 2,784 |
| Jun | 0.2677 | 0.2730 | 0.2903 | 1,134 | 0.0494 | 0.0483 | 0.0522 | 2,369 |
| Jul | 0.2554 | 0.2550 | 0.2731 | 1,221 | 0.0269 | 0.0269 | 0.0312 | 3,112 |
| Aug | 0.2137 | 0.2148 | 0.2401 | 1,669 | 0.0386 | 0.0387 | 0.0389 | 2,990 |
| Sep | 0.1921 | 0.1921 | 0.2243 | 1,737 | 0.0389 | 0.0389 | 0.0372 | 2,561 |
| Oct | 0.1765 | 0.1764 | 0.1988 | 1,831 | 0.0240 | 0.024 | 0.0267 | 3,127 |
| Nov | 0.1481 | 0.1523 | 0.1711 | 1,781 | 0.0089 | 0.0089 | 0.0122 | 3,585 |
| Dec | 0.1390 | 0.1411 | 0.1551 | 1,884 | 0.0128 | 0.0128 | 0.0127 | 3,366 |
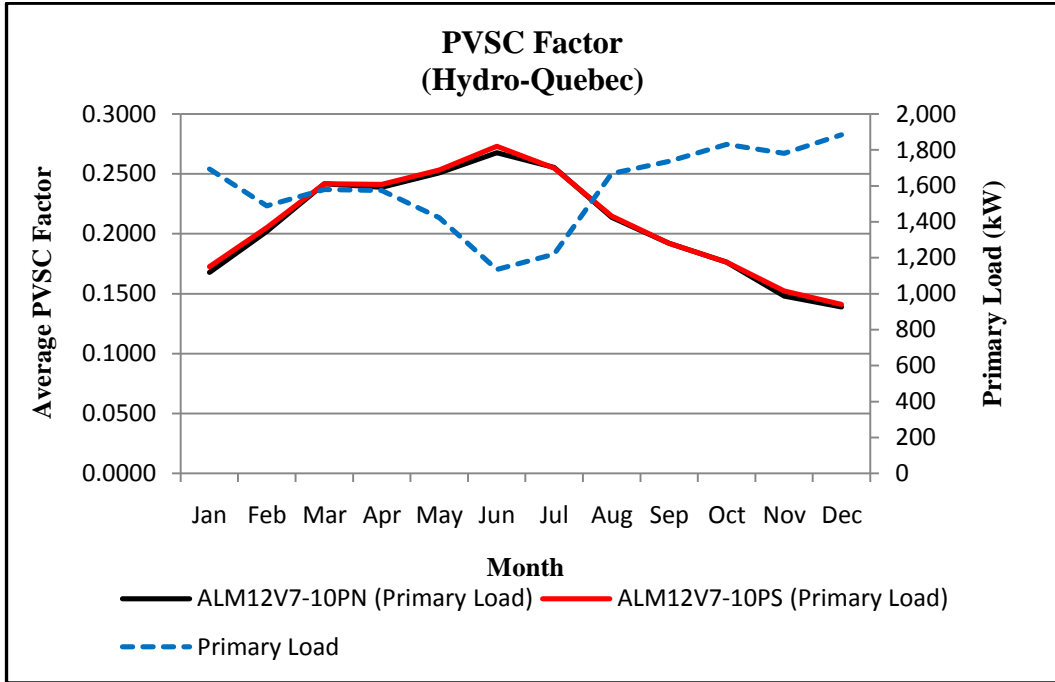
**Figure 28: Average PVSC Factor: New & Second Life Batteries (Hydro-Quebec)**
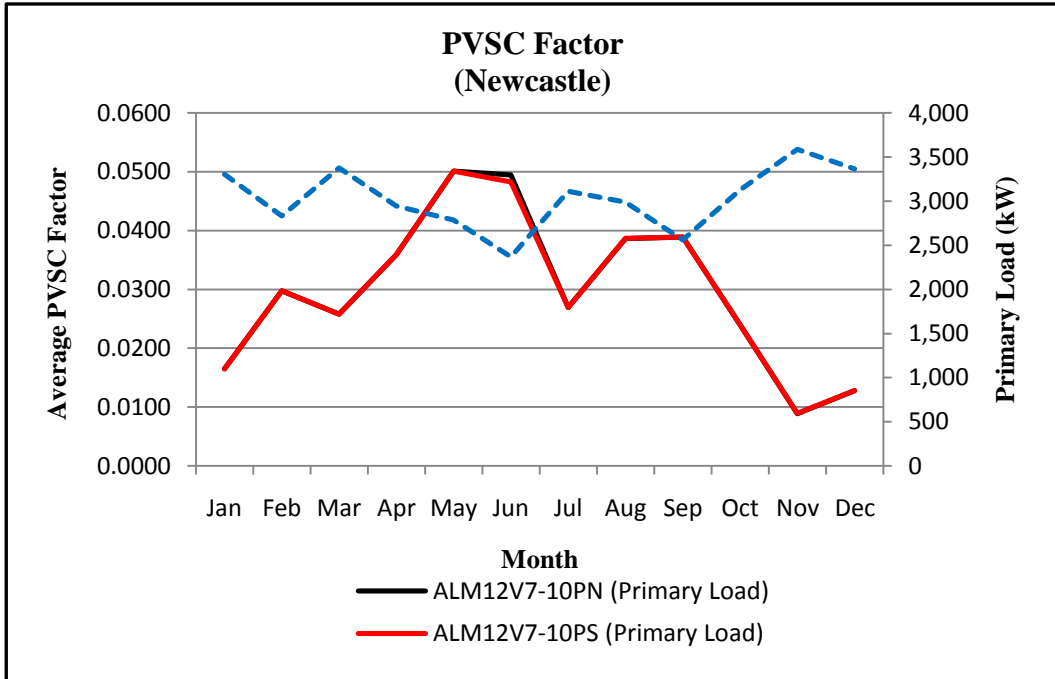


**Figure 29: Average PVSC Factor: New & Second Life Batteries (Newcastle)**

Moreover, the PVSC factors for the scenarios where deferrable loads are used are shown in Figure 30 and Figure 31.
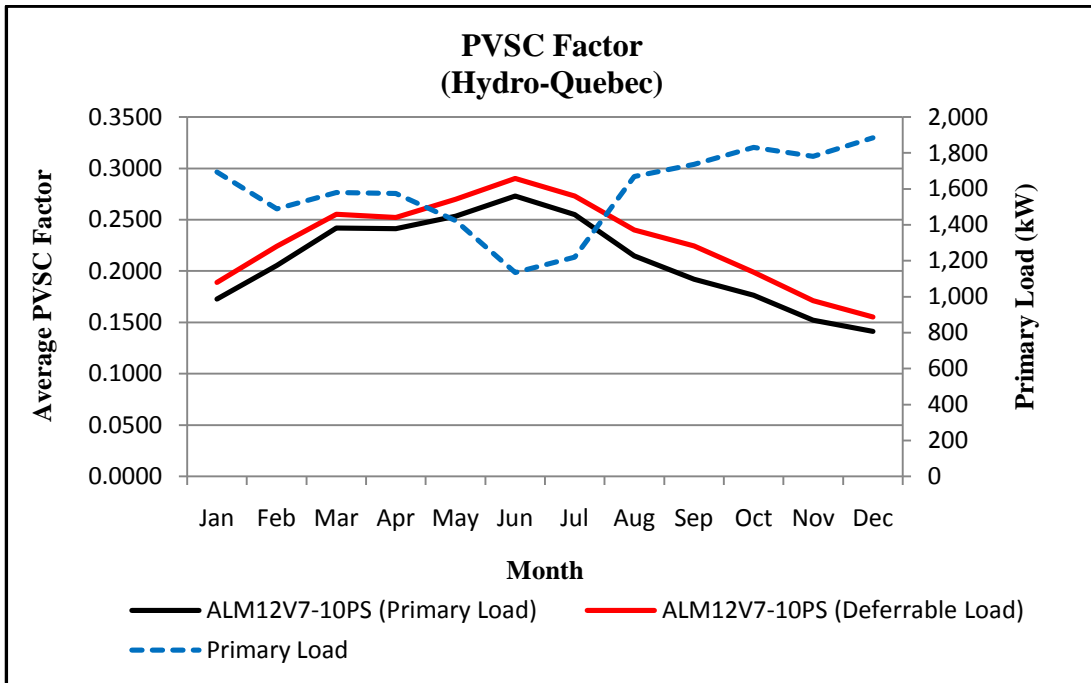
**Figure 30: Average PVSC Factor: Deferrable Loads (Hydro-Quebec)**
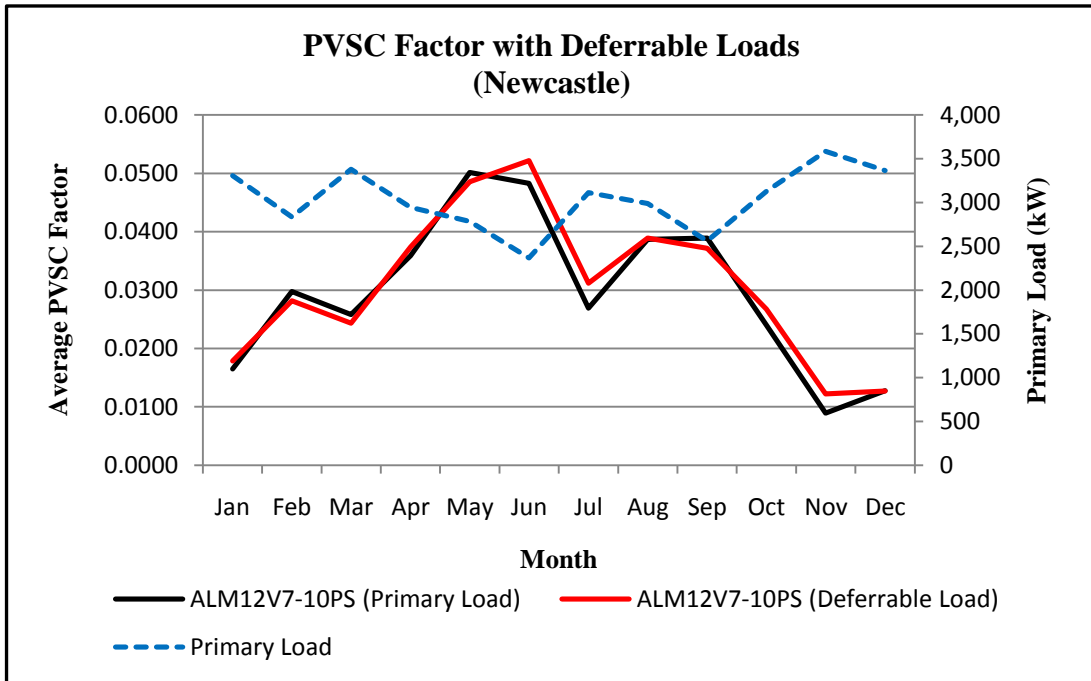


**Figure 31: Average PVSC Factor: Deferrable Loads (Newcastle)**

By inspection, the use of a new or second-life LFP battery does not impact upon the

PVSC factors with the high loads at both sites limiting the amount of the load served by

the solar and battery system. The low PVSC factors can be attributable to the high load and small-size solar array and battery combination at each site. Deferring loads to be served at a later time can increase the amount of PVSC but this is contingent on the prevailing load conditions. The higher PVSC factor measured at Hydro-Quebec can be attributed to the higher levels of solar radiation at that site. The average annual solar radiation at Hydro-Quebec (68.51 kWh/m$^2$/year) was about 2 times that at Newcastle (32.44kWh/m$^2$/year) resulting in an increase of 7.5 times the amount of PVSC. The fact that the PVSC factor is dependent on both the availability of solar energy and the load demand that is being served would suggest that in an environment characterised by low insolation and high load demand, the PVSC factor may be only one measure to consider when determining whether optimal use is made of the solar array and the battery system.

## 5.5    HOMER Anomalies

Where there is sufficient solar and battery power available this would usually be used to serve the load.  However, as illustrated in Figure 32, the results suggest that the energy from the solar array was discarded as "excess energy".  The reason why this occurs is because the amount of solar and battery power, on its own or in combination, at any given moment must be greater than the load that has to be served at the time [55].  If it is not, HOMER will dispatch other power sources that are available to serve the load.
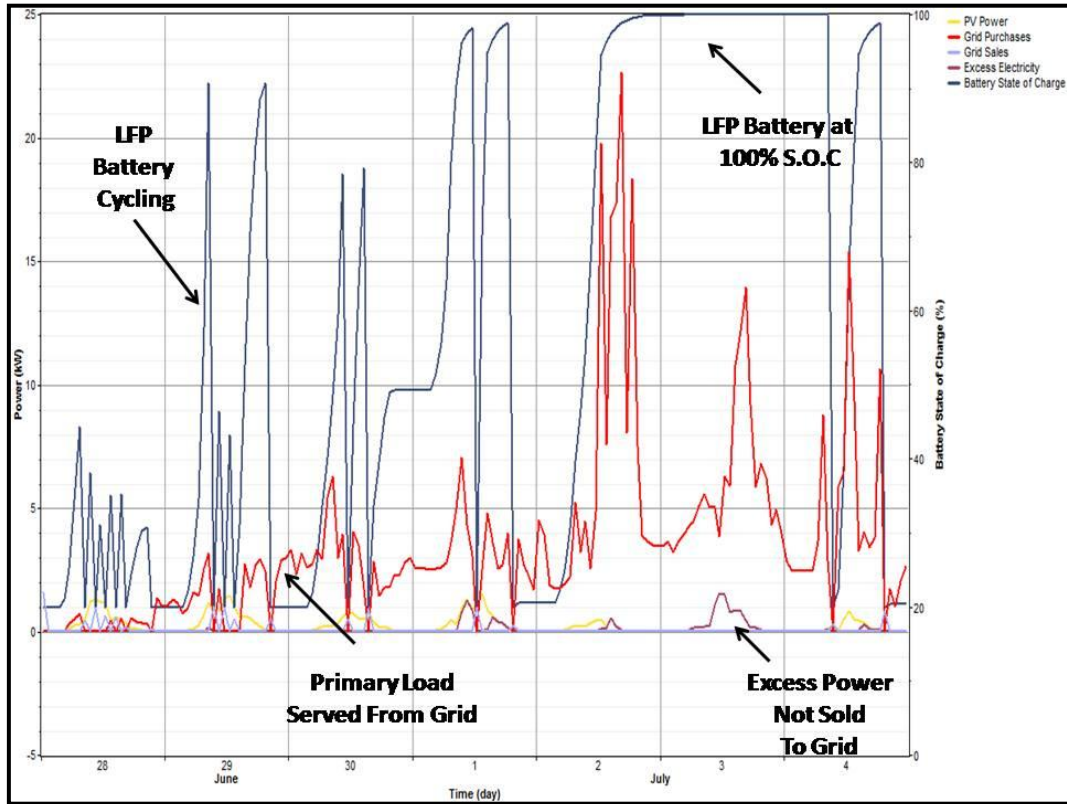


**Figure 32: HOMER Excess Power Anomaly (Newcastle)**

Furthermore, as illustrated in Figure 33, there are instances where the SOC remains at 100% even though there is sufficient capacity to serve the load.  As such, HOMER only

serves the load when there is sufficient battery power to serve the primary load either on its own or in combination with the solar array. Alternately, if the load is much greater than the amount of power available from the battery, HOMER will import the power from the grid to serve the load. When this happens, the battery is charged to its maximum by the solar array where it remains at 100% SOC until the load can be met by power from the battery.

| Date | End Time | Solar Radiation (kW/m2) | Incident Solar (kW/m2) | Ambient Temperature (°C) | Cell Temperature (°C) | AC Prim. Load (kW) | PV Power (kW) | Grid Purchases (kW) | Grid Sales (kW) | Excess Electricity (kW) | Inverter Input (kW) | Inverter Output (kW) | Rectifier Input (kW) | Rectifier Output (kW) | Battery Input (kW) | Battery SOC (%) | Battery Energy ($/kWh) |
|---|---|---|---|---|---|---|---|---|---|---|---|---|---|---|---|---|---|
| Jul 13 | 13:00 | 0.223 | 0.19 | 20.1 | 23.6 | 3.9 | 0.36 | 3.9 | 0.00 | 0.31 | 0.00 | 0.00 | 0.00 | 0.00 | 0.05 | 96 | 0.00 |
| Jul 13 | 14:00 | 0.101 | 0.08 | 20.1 | 21.7 | 3.4 | 0.16 | 3.4 | 0.00 | 0.13 | 0.00 | 0.00 | 0.00 | 0.00 | 0.04 | 98 | 0.00 |
| Jul 13 | 15:00 | 0.216 | 0.18 | 20.1 | 23.5 | 5.6 | 0.35 | 5.6 | 0.00 | 0.33 | 0.00 | 0.00 | 0.00 | 0.00 | 0.02 | 98 | 0.00 |
| Jul 13 | 16:00 | 0.166 | 0.14 | 20.1 | 22.7 | 5.2 | 0.27 | 5.2 | 0.00 | 0.25 | 0.00 | 0.00 | 0.00 | 0.00 | 0.02 | 99 | 0.00 |
| Jul 13 | 17:00 | 0.147 | 0.12 | 20.1 | 22.4 | 3.7 | 0.24 | 3.7 | 0.00 | 0.23 | 0.00 | 0.00 | 0.00 | 0.00 | 0.01 | 99 | 0.00 |
| Jul 13 | 18:00 | 0.068 | 0.06 | 20.1 | 21.1 | 3.6 | 0.11 | 3.6 | 0.00 | 0.10 | 0.00 | 0.00 | 0.00 | 0.00 | 0.01 | 99 | 0.00 |
| Jul 13 | 19:00 | 0.070 | 0.06 | 20.1 | 21.2 | 3.5 | 0.11 | 3.5 | 0.00 | 0.11 | 0.00 | 0.00 | 0.00 | 0.00 | 0.01 | 100 | 0.00 |
| Jul 13 | 20:00 | 0.015 | 0.01 | 20.1 | 20.3 | 3.8 | 0.02 | 3.8 | 0.00 | 0.02 | 0.00 | 0.00 | 0.00 | 0.00 | 0.00 | 100 | 0.00 |
| Jul 13 | 21:00 | 0.009 | 0.01 | 20.1 | 20.2 | 3.0 | 0.01 | 3.0 | 0.00 | 0.01 | 0.00 | 0.00 | 0.00 | 0.00 | 0.00 | 100 | 0.00 |
| Jul 13 | 22:00 | 0.000 | 0.00 | 20.1 | 20.1 | 6.1 | 0.00 | 6.1 | 0.00 | 0.00 | 0.00 | 0.00 | 0.00 | 0.00 | 0.00 | 100 | 0.00 |
| Jul 13 | 23:00 | 0.000 | 0.00 | 20.1 | 20.1 | 7.0 | 0.00 | 7.0 | 0.00 | 0.00 | 0.00 | 0.00 | 0.00 | 0.00 | 0.00 | 100 | 0.00 |
| Jul 14 | 0:00 | 0.000 | 0.00 | 20.1 | 20.1 | 3.0 | 0.00 | 3.0 | 0.00 | 0.00 | 0.00 | 0.00 | 0.00 | 0.00 | 0.00 | 100 | 0.00 |
| Jul 14 | 1:00 | 0.000 | 0.00 | 19.6 | 19.6 | 2.6 | 0.00 | 2.6 | 0.00 | 0.00 | 0.00 | 0.00 | 0.00 | 0.00 | 0.00 | 100 | 0.00 |
| Jul 14 | 2:00 | 0.000 | 0.00 | 19.6 | 19.6 | 2.5 | 0.00 | 2.5 | 0.00 | 0.00 | 0.00 | 0.00 | 0.00 | 0.00 | 0.00 | 100 | 0.00 |
| Jul 14 | 3:00 | 0.000 | 0.00 | 19.6 | 19.6 | 2.6 | 0.00 | 2.6 | 0.00 | 0.00 | 0.00 | 0.00 | 0.00 | 0.00 | 0.00 | 100 | 0.00 |
| Jul 14 | 4:00 | 0.000 | 0.00 | 19.6 | 19.6 | 2.6 | 0.00 | 2.6 | 0.00 | 0.00 | 0.00 | 0.00 | 0.00 | 0.00 | 0.00 | 100 | 0.00 |
| Jul 14 | 5:00 | 0.046 | 0.03 | 19.6 | 20.1 | 2.6 | 0.05 | 2.6 | 0.00 | 0.05 | 0.00 | 0.00 | 0.00 | 0.00 | 0.00 | 100 | 0.00 |
| Jul 14 | 6:00 | 0.134 | 0.07 | 19.6 | 20.9 | 2.7 | 0.14 | 2.7 | 0.00 | 0.14 | 0.00 | 0.00 | 0.00 | 0.00 | 0.00 | 100 | 0.00 |
| Jul 14 | 7:00 | 0.286 | 0.12 | 19.6 | 21.7 | 3.0 | 0.23 | 3.0 | 0.00 | 0.23 | 0.00 | 0.00 | 0.00 | 0.00 | 0.00 | 100 | 0.00 |
| Jul 14 | 8:00 | 0.363 | 0.28 | 19.6 | 24.6 | 6.2 | 0.53 | 6.2 | 0.00 | 0.53 | 0.00 | 0.00 | 0.00 | 0.00 | 0.00 | 100 | 0.00 |
| Jul 14 | 9:00 | 0.526 | 0.48 | 19.6 | 28.4 | 5.9 | 0.91 | 5.9 | 0.00 | 0.91 | 0.00 | 0.00 | 0.00 | 0.00 | 0.00 | 100 | 0.00 |
| Jul 14 | 10:00 | 0.480 | 0.46 | 19.6 | 28.0 | 8.2 | 0.87 | 8.2 | 0.00 | 0.87 | 0.00 | 0.00 | 0.00 | 0.00 | 0.00 | 100 | 0.00 |
| Jul 14 | 11:00 | 0.817 | 0.90 | 19.6 | 36.1 | 9.4 | 1.66 | 9.4 | 0.00 | 1.66 | 0.00 | 0.00 | 0.00 | 0.00 | 0.00 | 100 | 0.00 |
| Jul 14 | 12:00 | 0.698 | 0.76 | 19.6 | 33.6 | 5.6 | 1.43 | 5.6 | 0.00 | 1.43 | 0.00 | 0.00 | 0.00 | 0.00 | 0.00 | 100 | 0.00 |
| Jul 14 | 13:00 | 0.754 | 0.84 | 19.6 | 35.1 | 4.1 | 1.57 | 4.1 | 0.00 | 1.57 | 0.00 | 0.00 | 0.00 | 0.00 | 0.00 | 100 | 0.00 |
| Jul 14 | 14:00 | 0.804 | 0.89 | 19.6 | 36.1 | 5.2 | 1.66 | 5.2 | 0.00 | 1.66 | 0.00 | 0.00 | 0.00 | 0.00 | 0.00 | 100 | 0.00 |
| Jul 14 | 15:00 | 0.567 | 0.57 | 19.6 | 30.1 | 7.7 | 1.08 | 7.7 | 0.00 | 1.08 | 0.00 | 0.00 | 0.00 | 0.00 | 0.00 | 100 | 0.00 |
| Jul 14 | 16:00 | 0.371 | 0.33 | 19.6 | 25.7 | 17.6 | 0.64 | 17.6 | 0.00 | 0.64 | 0.00 | 0.00 | 0.00 | 0.00 | 0.00 | 100 | 0.00 |
| Jul 14 | 17:00 | 0.365 | 0.31 | 19.6 | 25.2 | 4.5 | 0.59 | 4.5 | 0.00 | 0.59 | 0.00 | 0.00 | 0.00 | 0.00 | 0.00 | 100 | 0.00 |
| Jul 14 | 18:00 | 0.288 | 0.19 | 19.6 | 23.0 | 4.5 | 0.36 | 4.5 | 0.00 | 0.36 | 0.00 | 0.00 | 0.00 | 0.00 | 0.00 | 100 | 0.00 |
| Jul 14 | 19:00 | 0.179 | 0.08 | 19.6 | 21.1 | 2.7 | 0.16 | 2.7 | 0.00 | 0.16 | 0.00 | 0.00 | 0.00 | 0.00 | 0.00 | 100 | 0.00 |
| Jul 14 | 20:00 | 0.078 | 0.04 | 19.6 | 20.4 | 2.7 | 0.09 | 2.7 | 0.00 | 0.09 | 0.00 | 0.00 | 0.00 | 0.00 | 0.00 | 100 | 0.00 |
| Jul 14 | 21:00 | 0.008 | 0.01 | 19.6 | 19.7 | 3.5 | 0.01 | 3.5 | 0.00 | 0.01 | 0.00 | 0.00 | 0.00 | 0.00 | 0.00 | 100 | 0.00 |
| Jul 14 | 22:00 | 0.000 | 0.00 | 19.6 | 19.6 | 5.0 | 0.00 | 5.0 | 0.00 | 0.00 | 0.00 | 0.00 | 0.00 | 0.00 | 0.00 | 100 | 0.00 |
| Jul 14 | 23:00 | 0.000 | 0.00 | 19.6 | 19.6 | 5.4 | 0.00 | 5.4 | 0.00 | 0.00 | 0.00 | 0.00 | 0.00 | 0.00 | 0.00 | 100 | 0.00 |
| Jul 15 | 0:00 | 0.000 | 0.00 | 19.6 | 19.6 | 3.9 | 0.00 | 3.9 | 0.00 | 0.00 | 0.00 | 0.00 | 0.00 | 0.00 | 0.00 | 100 | 0.00 |
| Jul 15 | 1:00 | 0.000 | 0.00 | 17.5 | 17.5 | 2.6 | 0.00 | 2.6 | 0.00 | 0.00 | 0.00 | 0.00 | 0.00 | 0.00 | 0.00 | 100 | 0.00 |
| Jul 15 | 2:00 | 0.000 | 0.00 | 17.5 | 17.5 | 2.5 | 0.00 | 2.5 | 0.00 | 0.00 | 0.00 | 0.00 | 0.00 | 0.00 | 0.00 | 100 | 0.00 |
| Jul 15 | 3:00 | 0.000 | 0.00 | 17.5 | 17.5 | 2.6 | 0.00 | 2.6 | 0.00 | 0.00 | 0.00 | 0.00 | 0.00 | 0.00 | 0.00 | 100 | 0.00 |
| Jul 15 | 4:00 | 0.000 | 0.00 | 17.5 | 17.5 | 2.5 | 0.00 | 2.5 | 0.00 | 0.00 | 0.00 | 0.00 | 0.00 | 0.00 | 0.00 | 100 | 0.00 |
| Jul 15 | 5:00 | 0.039 | 0.03 | 17.5 | 18.0 | 2.6 | 0.05 | 2.6 | 0.00 | 0.05 | 0.00 | 0.00 | 0.00 | 0.00 | 0.00 | 100 | 0.00 |
| Jul 15 | 6:00 | 0.096 | 0.07 | 17.5 | 18.8 | 2.6 | 0.14 | 2.6 | 0.00 | 0.14 | 0.00 | 0.00 | 0.00 | 0.00 | 0.00 | 100 | 0.00 |
| Jul 15 | 7:00 | 0.255 | 0.13 | 17.5 | 19.8 | 2.8 | 0.25 | 2.8 | 0.00 | 0.25 | 0.00 | 0.00 | 0.00 | 0.00 | 0.00 | 100 | 0.00 |
| Jul 15 | 8:00 | 0.188 | 0.16 | 17.5 | 20.4 | 3.6 | 0.31 | 3.6 | 0.00 | 0.31 | 0.00 | 0.00 | 0.00 | 0.00 | 0.00 | 100 | 0.00 |
| Jul 15 | 9:00 | 0.405 | 0.36 | 17.5 | 24.1 | 5.0 | 0.70 | 5.0 | 0.00 | 0.70 | 0.00 | 0.00 | 0.00 | 0.00 | 0.00 | 100 | 0.00 |
| Jul 15 | 10:00 | 0.598 | 0.60 | 17.5 | 28.6 | 6.0 | 1.15 | 6.0 | 0.00 | 1.15 | 0.00 | 0.00 | 0.00 | 0.00 | 0.00 | 100 | 0.00 |
| Jul 15 | 11:00 | 0.734 | 0.86 | 17.5 | 33.4 | 8.8 | 1.61 | 8.8 | 0.00 | 1.61 | 0.00 | 0.00 | 0.00 | 0.00 | 0.00 | 100 | 0.00 |

Figure 33: HOMER SOC Calculation Anomaly (Newcastle)

## 5.6   Further Simulation Work

There were evident limitations of using HOMER as a tool to simulate the operating environment of a PVSC system. The output from HOMER is determined by the

configuration of the PVSC.  For instance, a small converter would constrain the amount of power that is being transferred between the PV system and battery and the load. However, it is important to consider the fact that system components should as much as possible be reflective of the PV systems rather than ideal residential environments.  Not accounting for real life constraints can risk reducing the utility of the simulation results.

# Chapter 6: Key Findings

## 6.1 Conclusions

PV self-consumption (PSVC) systems are established to maximise the amount of solar power used to serve the load. The rationale for using a PVSC system is to ameliorate the mismatch between the time solar power is generated and when it is consumed. This is achieved by introducing an energy storage system into the operating environment to defer the use of solar power until when it is needed by the load.

In this project, it was shown that HOMER simulations could be used to provide insight into the operation of a PVSC system. Using a lithiated ion phosphate (LFP) battery as storage, it was shown that there were no significant differences between using a new or second-life battery to service the load in a PVSC system. A second-life battery rated at 80% capacity of a new one did not perform significantly differently to a new one. As indicated by the comparisons of the PVSC factors, the differences in the amount of PVSC were negligible. However, the use of the PVSC factor as a measure of the utilization of PVSC is highly dependent on the demand for power.

When operating within this system, the battery undergoes many charge-discharge cycles in a random and non-deterministic pattern. In turn, the charging and discharging of the battery will be dictated by the availability of solar power to charge the battery and the load demand that draws power from it. In these situations, LIBs like LFP batteries could be used so long as deep-cycling the battery does not comprise its safe use.

Finally, in spite of some anomalies with the HOMER program, the simulation was able to provide some insight into the operation of a PVSC system. For this project, assessing costs was not an explicit objective. However, the ability for HOMER to calculate the operational costs of such a system makes it useful to simulate scenarios where cost optimization is a priority.

## 6.2    Suggestions for Further Work

To ensure that the PVSC factor can provide insightful information about the operation of PVSC systems, there may be a need to standardise the conditions under which PVSC is measured. This includes the load environments measured from different residential and commercial settings. As such, this could improve the ability to assess the relative capability of combinations of solar and battery systems used for PVSC purposes.

Another important aspect of PVSC systems that would require further research is the effect of cycling on the electrochemistry of the LFP battery. This is because heavy cycling often results in capacity or power fade reducing the lifetime of the battery. Where a second-life battery is used, the tolerance to abuse may not be as great as a new one. As a consequence, further work might be directed towards investigating the capabilities of second-life LFP batteries thereby allowing more accurate PVSC models to be developed.

Finally, second-life LIBs might be suitable where the adoption of PVSC is cost-sensitive. For instance, this could include PVSC systems in emerging countries or non-metropolitan areas where access to resources is constrained and where the load demands originate from basic appliances. As such, further research into the abilities of second-life LIBs could be

beneficial in meeting the longer term needs of these communities.

# Chapter 7: References

[1]   H. Masheleni, Carelse., X.F., "Microcontroller Based Charge Controller For Stand-Alone Photovoltaic Systems," *Solar Energy,* vol. 61, pp. 225-330, 1997.

[2]   AT.Kearney, "Enabling The European Consumer To Generate Power For Self-Consumption," Sun Edison & Estudio Juridco Internacional 2011.

[3]   N. G. Nair, Niraj, "Battery Energy Storage Systems: Assessment for Small-Scale Renewable Energy Integration," *Energy & Buildings,* vol. 42, pp. 2124-2130, 2010.

[4]   S. M. Fitzpatrick, M, "Community Energy Storage Report," Advanced Energy, Raleigh, NC 27606-38702011.

[5]   L. A. Scheinbein, E.D, Jeffrey, "Chapter 11: Electric Power Distribution Systems," in *Distributed Generation: The Power Paradigm for the New Millennium*, A. M. a. K. Borbely, J.F. , Ed., ed: CRC Press, 2001, pp. 11.14-11.20.

[6]   L. Wagner, Froome, C & Foster J. (2011). *Modelling the Broader Deployment of Demand Side Management onto the Australian National Electricity Market*. Available: **http://igrid.net.au/resources/downloads/project2/journals/Wagner_USAEE_2011.pdf** Accessed: 11/10/2011.

[7]   J. Ledger, "Saft Lithium-Ion Battery Technology Selected to Provide Renewable Energy Storage for Sacramento Municipal Utility District Pilot Project," ed: SAFT Incorporated, 2010.

[8]   C. Marnay. (2010, 02/11/2011). *Microgrids: US Activities*. Available: **http://www.microgrids.eu/documents/Ch._Marnay_US_Activities-2.pdf** Accessed: 02/11/2011.

[9] M. Rawson. (2011). *SMUD PV and Smart Grid Pilot at Anatolia*. Available:

**http://www1.eere.energy.gov/solar/pdfs/highpenforum1-14_rawson_smud.pdf**

Accessed: 02/11/2011.

[10] M. DeAngelis. (2011). *Community Renewables & Integration At SMUD*.

Available: **http://cal-ires.ucdavis.edu/files/events/2011-resco-symposium/deangelis-**

**mike_cal-ires-resco-smud.pdf** Accessed: 02/09/2011

[11] M. Rawson. (2011). *PANEL 3: Utilities' Perspective of Energy Storage*. Available:

**http://www.energy.ca.gov/2011_energypolicy/documents/2011-04-**

**2_workshop/presentations/20_SMUD_Rawson_Panel_3.pdf** Accessed: 02/11/2011.

[12] Thomas, "Sunslates Product Information," A. E. S. Inc., Ed., ed, 2007.

[13] Alix, "Intensium 3," S. Incorporated, Ed., ed, 2010.

[14] A. U. Schmiegel, Knaup, P.,Meissner, A., Jehoulet, C., Schuh, H., Landau, M.,

Braun, M.,  Sauer, D.U. , Magnor D. &  Mohring, H.D., "The Sol-Ion System: A

Stationary PV Battery System," presented at the Conference IRES Berlin Voltwerk,

2010.

[15] *Sol-Ion Project: Purposes & Objectives*. Available: **http://www.sol-ion-**

**project.eu/sites/en/sol-ion-project/overview.html** Accessed: 02/11/2011.

[16] (Federal Ministry for the Environment (BMU)). *Renewable Energy Sources Act,*

*EEG, 2008*.

[17] *Sol-Ion Project: Partners*. Available: **http://www.sol-ion-**

**project.eu/sites/en/partners/E.ON** Accessed: 02/11/2011.

[18] B. K. Braun. M, Magnor D., Jossen. A, "Photovoltaic Self-Consumption In

Germany Using Lithium-Ion Storage To Increase Self-Consumed Photovoltaic Energy,"

presented at the 24th European Photovoltaic Solar Energy Conference, Hamburg, Germany, 2009.

[19] S. Lenoir, "Solar Europe Implementation Plan 2010-2012," European Photovoltaic Industry Association2010.

[20] F. Caricchi, Cresimbini, F., Capponi, G., Solero., L., "Study of Bi-Directional Buck-Boost Converter Topologies for Application in Electrical Vehicle Motor Drives," presented at the Applied Power Electronics Conference and Exposition, 1998.

[21] W. Woyke. (2011). *Options for Integrated Systems*. Available:**http://www.iea.org/work/2011/storage/Item4_EOn.pdf** Accessed: 11/10/2011.

[22] J. Raach. (2009). *Photovoltaics: Independent power supply or grid connection? The future starts with decentralized energy storage connected to the grid*. Available: **http://www.renewables-made-in** germany.com/fileadmin/publikationen_ veranstaltungsdoku/dokumente/PV_2009/de-PV-Taiwan-2009- Raach_property_pdf_bereich_renewables_sprache_de_rwb_true.pdf Accessed: 02/11/2011.

[23] N. Kreutzer, "Self-Supply System Based on PV," S. S. T. AG, Ed., ed. Dresden, Germany: LVDC Workshop, 2011.

[24] M. Lippert. (2009). *Residential PV System Combined with Energy Storage: Sol-Ion & Other Examples*. Available: **http://www.sol-ion-project.eu/export/sites/ default/en/_data/publications/mediatheque-files/Conf_EPIA_Brussels _SAFT_0209.pdf** Accessed: 02/11/2011

[25] M. Castillo-Cargigal, Gutierrez. A, Monasterio, F, Caamano-Martin, E., Masa-Bote, D., Porro, P., Matallanas, J and Jimenenz-Leube, J., "Self-Consumption of PV Electricity With Active Demand Side Management: The GEDELOS-System," presented at the 25th European Photovoltaic Solar Energy Conference Exhibition, Valencia, Spain, 2010.

[26] M. Castillo-Cargigal, Gutierrez. A, Monasterio-Huelin, F, Caamano-Martin, E., Masa, D. & Jimenez-Leube, J, "A Semi-Distributed Electric Demand-Side Management System With PV Generation For Self-Consumption Enhancement," *Energy Conversion and Management,* vol. 52, pp. 2659-2666, 2011.

[27] J. Dahn, Ehrlich, G., "Chapter 26: Lithium Ion Batteries," in *Linden's Handbook of Batteries*, T. Freddy, Ed., 4 ed: McGraw Hill, 2002, pp. 26.1-26.79.

[28] J. Dahn, Ehrlich, G., "Chapter 14: Lithium Primary Batteries," in *Linden's Handbook of Batteries*, T. Freddy, Ed., 4 ed: McGraw Hill, 2002, pp. 14.69-14.89.

[29] *Chemistry Tutorial: The Nernst Equation*. Available: **http://www.ausetute.com.au/nernst.html** Accessed: 6/06/2012

[30] R. Yazami, "Chapter 5: Thermodynamics of Electrode Materials for Lithium-Ion Batteries," in *Lithium Ion Rechargeable Batteries*, K. Ozawa, Ed., ed: Wiley-Vch Verlag GmbH, 2009, pp. 67-68.

[31] J. Vetter, Novak, P., Wagner, M.R., Veit, C., Moller, K.C., Besenhard, J.O., Winter, M., Wohlfahrt-Mehrens, M.,Vogler, C. and Hammouche, A. , "Ageing Mechanisms in Lithium-Ion Batteries," *Journal of Power Sources,* pp. 269-281, 2005.

[32] K. Aifantis, "Chapter 6: Next Generation Anodes for Secondary Li-ion Batteries " in *High Energy Lithium Batteries*, H. Aifantis K., S., Kumar, R., Ed., ed: Wiley-Vch Verlag GmbH, 2010, pp. 129-130.

[33] R. Alcantara, Lavela,P., Perez-Vicente, C., Tirado., J "Chapter 3: Anode Materials for Lithium-Ion Batteries," in *Lithium-Ion Batteries Advanced Materials and Technologies*, J. Yuan, Liu, X. and Zhang, H., Ed., ed: CRC Press, 2011, p. 100.

[34] J. Dahn, Ehrlich, G., "Chapter 26: Lithium Ion Batteries," in *Linden's Handbook of Batteries*, T. Freddy, Ed., 4 ed: McGraw Hill, 2002, p. 26.30.

[35] Z. Bakenov, Taniguchi. I, "Chapter 2: Cathode Material for Lithium-Ion Batteries," in *Lithium-Ion Batteries Advanced Materials and Technologies*, J. Yuan, Liu, X. and Zhang, H., Ed., ed: Wiley-Vch Vera GM, 2010, pp. 51-95.

[36] P. P. Prosini, "Chapter 1: Electrode Materials for Lithium-Ion Batteries," in *Iron Phosphate Materials as Cathodes for Lithium Batteries*, ed London: Springer-Verlag London Limited, 2011, pp. 1-12.

[37] A. K. Padhi, Nanjundaswamy, K.S., Gooodenough, J.B.,, "Phospho-olivines as Positive-Electrode Materials for Rechargeable Lithium Batteries," *Journal of Electrochemical Society,* vol. 144, pp. 1188-1194, 1997.

[38] W. Jiayuan, Zechang, S. and Xuezhe, W., "Performance and Characteristic Research in LiFePO4 Battery for Electric Vehicles Applications," presented at the Vehicle Power and Propulsion Conference, 2009. VPPC '09. IEEE, 2009.

[39] J. Dahn, Ehrlich, G., "Chapter 26: Lithium Ion Batteries," in *Linden's Handbook of Batteries*, T. Freddy, Ed., 4 ed: McGraw Hill, 2002, p. 26.47.

[40] M. Takahashi, Tobishima, S., Takei, K., Sakurai, Y. , "Characterization of LiFePO4 as the Cathode Material For Rechargeable Lithium Batteries," *Journal of Power Sources,* pp. 508-511, 2001.

[41] P. P. Prosini, "Chapter 6: Nano-Crystalline LiFePO4," in *Iron Phosphate Materials as Cathodes for Lithium Batteries*, ed London: Springer-Verlag London Limited, 2011, pp. 47-49.

[42] "High Energy Lithium Ion Cell VL 45 E Cell," S. Incorporated, Ed., ed.

[43] Y. Z. Dong, Zhao,Y.M. and  Duan, H., "Crystal Structure and Lithium Electrochemical Extraction Properties of Olivine Type LiFePO4," *Materials Chemistry and Physics,* pp. 756-760, 2011.

[44] H.-S. Kim, Cho, Byung-Won & Cho, Won-I., "Cycling Performance of LiFePO4 Cathode Material for Lithium Secondary Batteries," *Journal of Power Sources* pp. 235-239, 2004.

[45] J. Hassoun, Croce, Fausto., Hong, Inchul., Scrosati, B, "Lithium-iron Battery: Fe203 anode versus LiFePO4 Cathode," *Electrochemistry Communications,* vol. 13, pp. 228-231, 2011.

[46] A. S. Andersson, Thomas., J.O., "The Source of First Cycle Capacity Loss in LiFePo4," *Journal of Power Sources,* vol. 97-98, pp. 498-502, 2001.

[47] "High Power Lithium Ion ANR26650m1," ed, 2006.

[48] X. H. Rui, Jin, Y. ,  Feng, X.Y., Zhang, L.C, Chen, C.H., "A Comparative Study on the Low-Temperature Performance of LiFePO4 /C and Li3V2(PO4)3/C Cathodes for Lithium-Ion Batteries," *Journal of Power Sources,* pp. 2109-2114, 2011.

[49] H. Xiaosong, Shengbo, Li and Peng, Hui, "A Comparative Study of Equivalent Circuit Models for Li-ion Batteries," *Journal of Power Sources,* vol. 198, pp. 359-367, 2012.

[50] J. C. Forman, Moura, Scott J.,Stein, Jeffrey L., and Fathy, Hosnam K, "Genetic Idenitification and Fisher Identifiability Analysis of the Doyle-Fuller-Newman Model from Experimental Cycling of a LiFePO4 Cell," *Journal of Power Sources,* vol. 210, pp. 263-275, 2012.

[51] K. Nunotani, Yoshida, F., Kamiya, Y., Daisho, Y., Kazuo, K., Kono, M. and Matsuo, H., "Development and Performance Evaluation of Lithium Iron Phosphate Battery with Superior Rapid Charging Performance- Second Report; Evaluation of Battery Capacity Loss Characteristics," presented at the IEEE Vehicle Power and Propulsion Conference 2011, 2011.

[52] F. Codeca, Savaresi, Sergio M., Rizzoni G., "On Battery State of Charges Estimation : A New Mixed Algorithm," presented at the 17th IEEE International Conference on Control Applications, San Antonio, Texas USA, 2008.

[53] S. B. Peterson, Apt, Jay and Whiteacre, J.F., "Lithium-ion Battery Cell Degradation Resulting from Realistic Vehicle and Vehicle-to-Grid Utilization," *Journal of Power Sources,* vol. 195, 2011.

[54] J. Wang, Liu, P., Hicks-Garner, J., Sherman, E., Soukiazian, S., Verbrugge., M, Tataria., H, Musser, J., Finamore., P., "Cycle Life for Graphite LiFEPO4 Cells," *Journal of Power Sources,* vol. 196, pp. 3942-3948, 2011.

[55] T. Lambert, "Micropower System Modeling With HOMER," in *Integration of Alternative Source of Energy*, ed: John Wiley & Sons, Inc., 2006, pp. 379-417.

[56] I. Knight, Kreutzer, N. (2010). *The Simulation of Building Integrated Fuel Cell and Other Cogeneration Systems*. Available: **http://www.iea-annex54.org/annex42/data.html** Accessed: 20/4/2012.

[57] *NASA Surface Meterology and Solar Energy*. Available: **http://eosweb.larc.nasa.gov/sse/** Accessed: 29/4/2012.

[58] C. Jardine, Bergman, N. (2009). *The Status of the UK Domestic PV Market - A Review of the Impact of the Low Carbon Buildings Programme*. Available: **http://www.eci.ox.ac.uk/publications/downloads/jardine09-pvprogramme.pdf** Accessed: 20/4/2012.

[59] V. Hamidi, Li, F., Robinson, F., "Demand Response in the UK's Domestic Sector," *Electric Power Systems Research,* vol. 79, pp. 1722-1726, 2009.

[60] V. a. F. Ugursal, A., "Residential Carbon Dioxide Emissions in Carbon," *Global Environmental Change,* vol. 8, pp. 263-373, 1998.

[61] "A123 Systems ALM 12V7 User's Guide,"  406017-001, 24th April 2012 2012.

[62] *Long-Lat.com*. Available: **http://www.lat-long.com** Accessed: 29/04/2012

[63] *National Bank Of Canada*. Available: **http://www.nbc.ca/bnc/cda/feeds/0,,divId-2_langId-1_navCode-9024,00.html#pretpersofixe** Accessed: 29/04/2012.

[64] *Rateinflation.com*. Available: **http://www.rateinflation.com/inflation-rate/usa-inflation-rate.php** Accessed: 29/04/2012.

[65] *Top 10 Loans UK-Clysdale Bank*. Available: **http://www.money.co.uk/loans.htm** Accessed: 29/04/2012

[66] *Oanda.com (Exchange Rates at 29/03/2012)*. Available: **http://www.oanda.com/currency/converter/** Accessed: 29/04/2012.

[67] *Sanyo Solar Panels*. Available: **http://www.shop.solar-wind.co.uk/acatalog/sanyo_solar_pv_panels.html** Accessed: 29/04/2012

[68] *SolaZone Grid Connected Power Inverters*. Available: **http://www.solazone.com.au/gridinvert.htm** Accessed: 29/04/2012

[69] *Aerooakku*. Available: **http://www.aeroakku.com/product_info.php/info/p452_A123-ALM-12V7.html** Accessed: 29/04/2012

[70] *Hydro-Quebec*. Available: **http://www.hydroquebec.com/residential/tarif-residentiel.html** Accessed: 29/04/2012

[71] *UK Power Co.* Available: **http://www.ukpower.co.uk/homeenergy** Accessed: 29/04/2012

[72] I. Cuthbert. *Domestic Behavioral Energy Use Advice – Exhaustive List*. Available: **http://www.energysavingtrust.org.uk/Media/Generate-your-own-energy/PDFs/FAQs-on-UK-Government-Feed-in-Tariffs** Accessed: 29/04/2012

[73] N. Agy, "HIT-N240-235-230-EN_f Product Specification," S. Incorporated, Ed., ed, 2010, pp. 1-2.

# Appendix 1

## A1.1  Implementation of HOMER Model

The specifications of the solar array at each site are shown in Figure 34 and Figure 35.
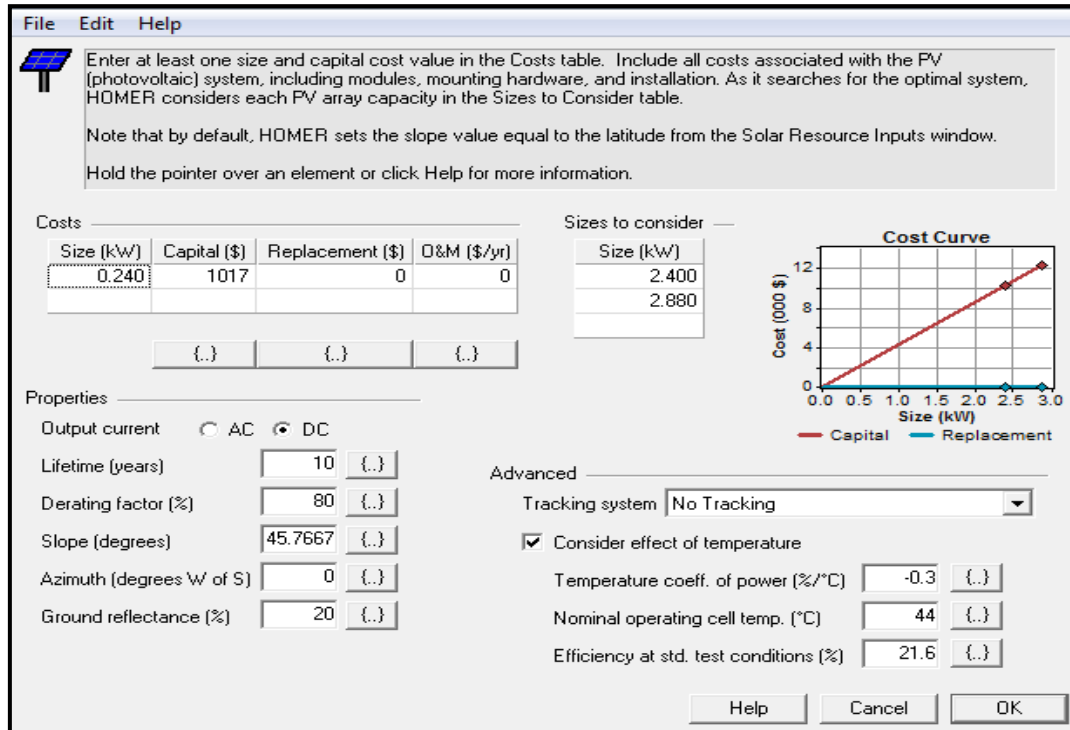


**Figure 34: Solar Panel Profile: Sanyo HITN240SE10 (Hydro-Quebec)**

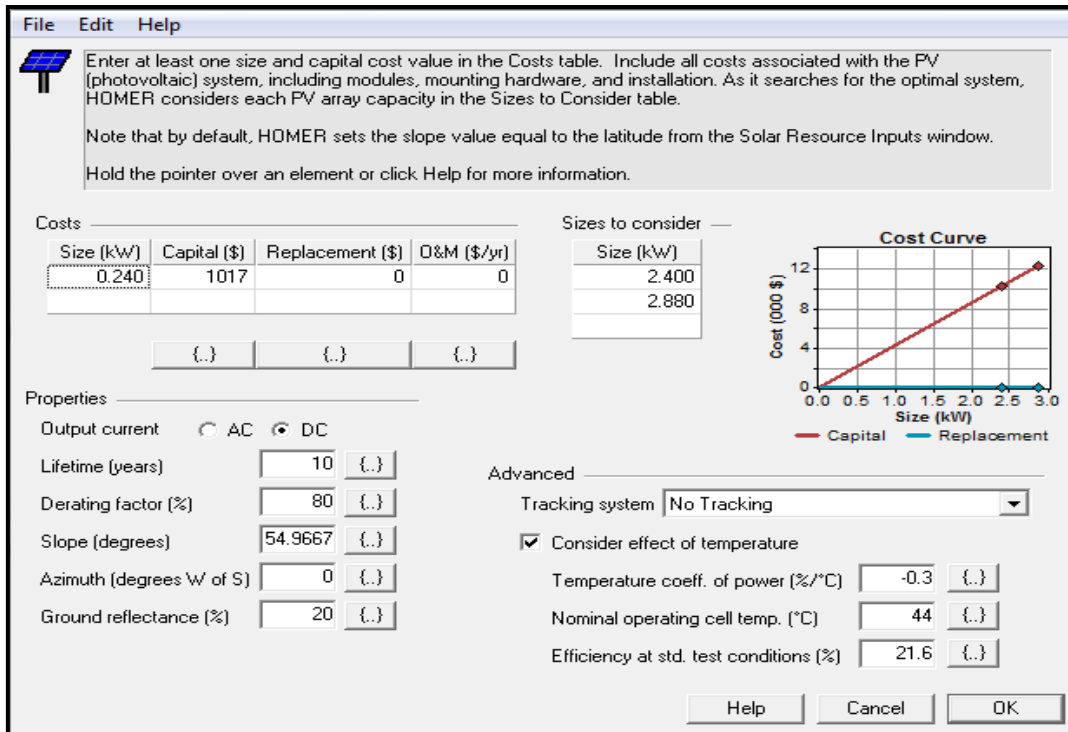**Source: HIT-N240-235-230-EN_froduct Specification [73]**

**Figure 35: Solar Panel Profile: Sanyo HITN240SE10 (Newcastle)**

**Source: HIT-N240-235-230-EN_froduct Specification [73]**

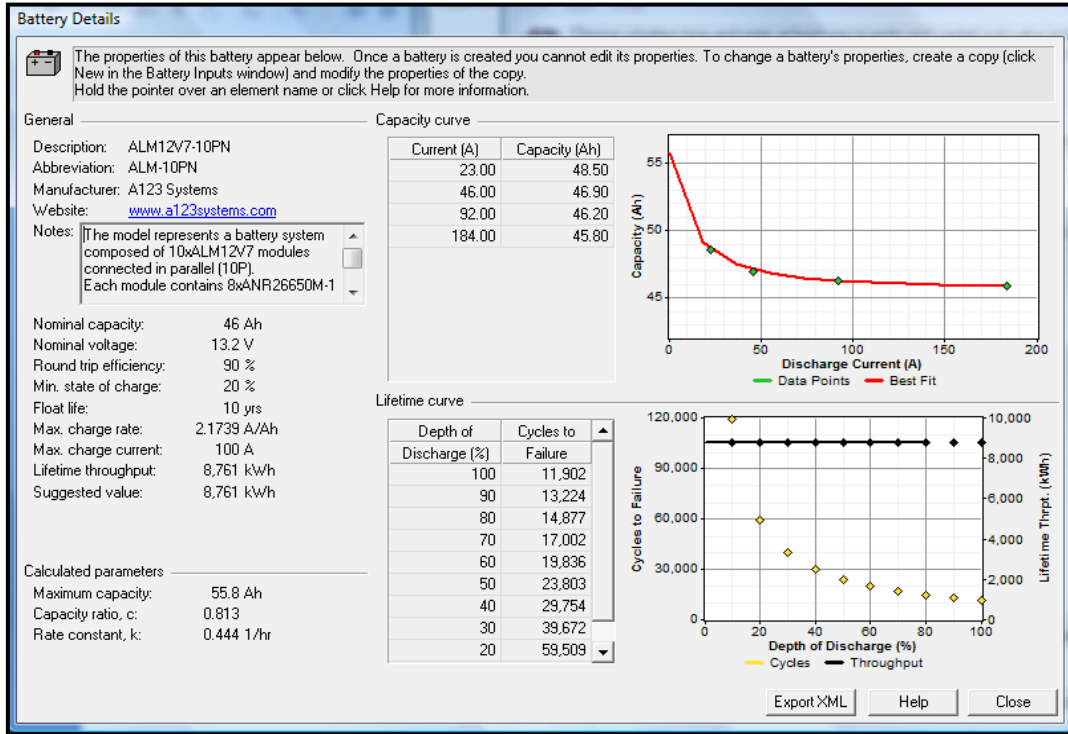The configuration for the new and second-life battery models are shown in Figure 36 and
Figure 37.



**Figure 36: ALM12V7-10PN Configuration**
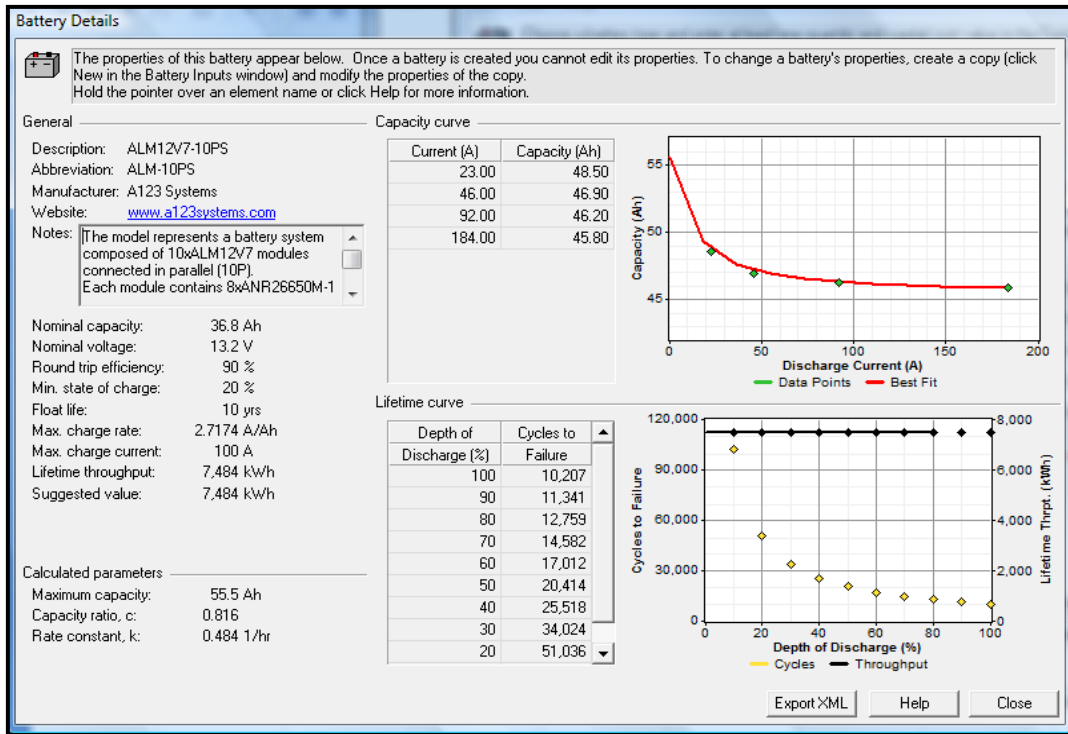


**Figure 37: ALM12V7-10PS Configuration**

The specifications for the converter are shown in Figure 38.
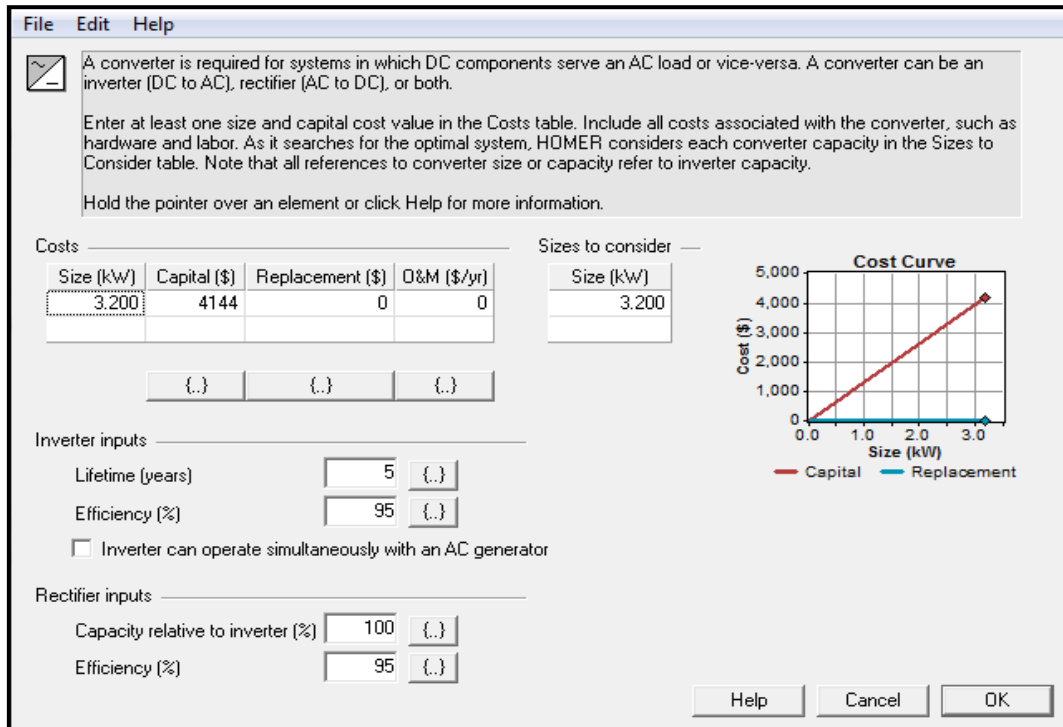


**Figure 38: Converter Specification**
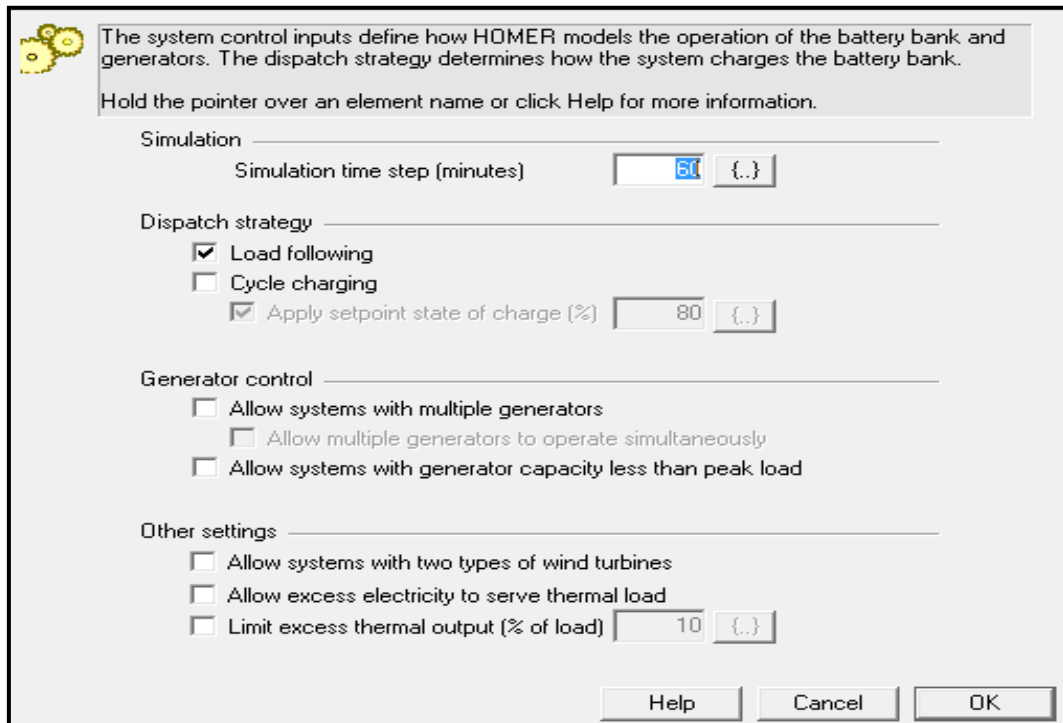
The control strategy adopted is shown in Figure 39.



**Figure 39: Simulation System Controls**

# Appendix 2

## A2.1 Battery Output Data

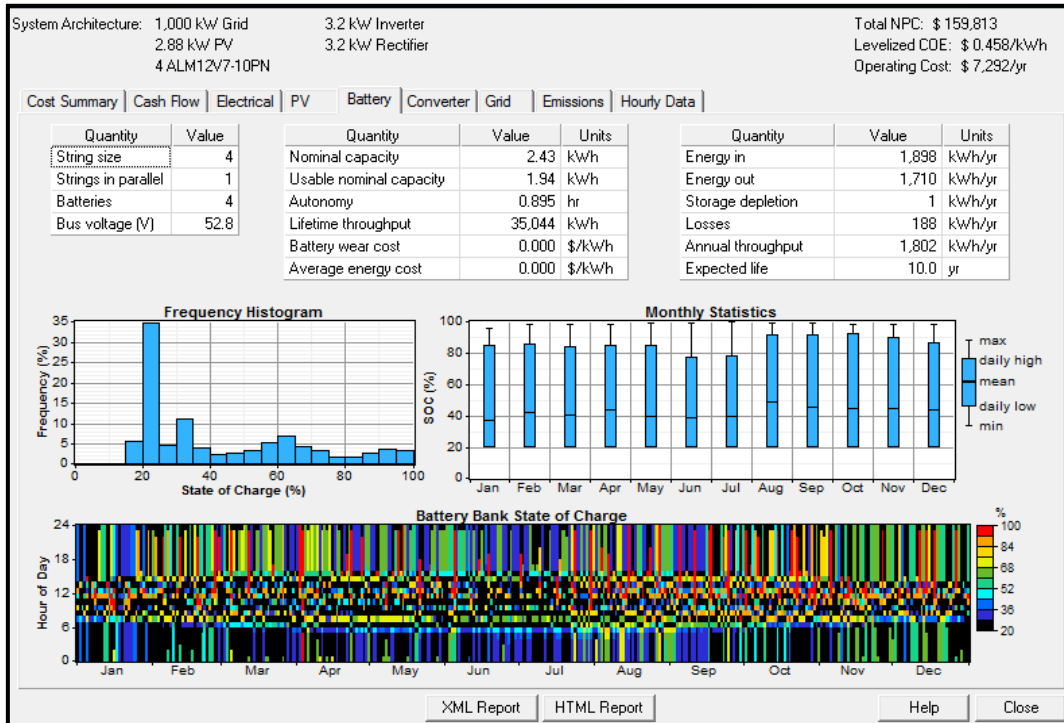The output for the battery performance is shown in Figure 40, Figure 41, Figure 42 and Figure 43.



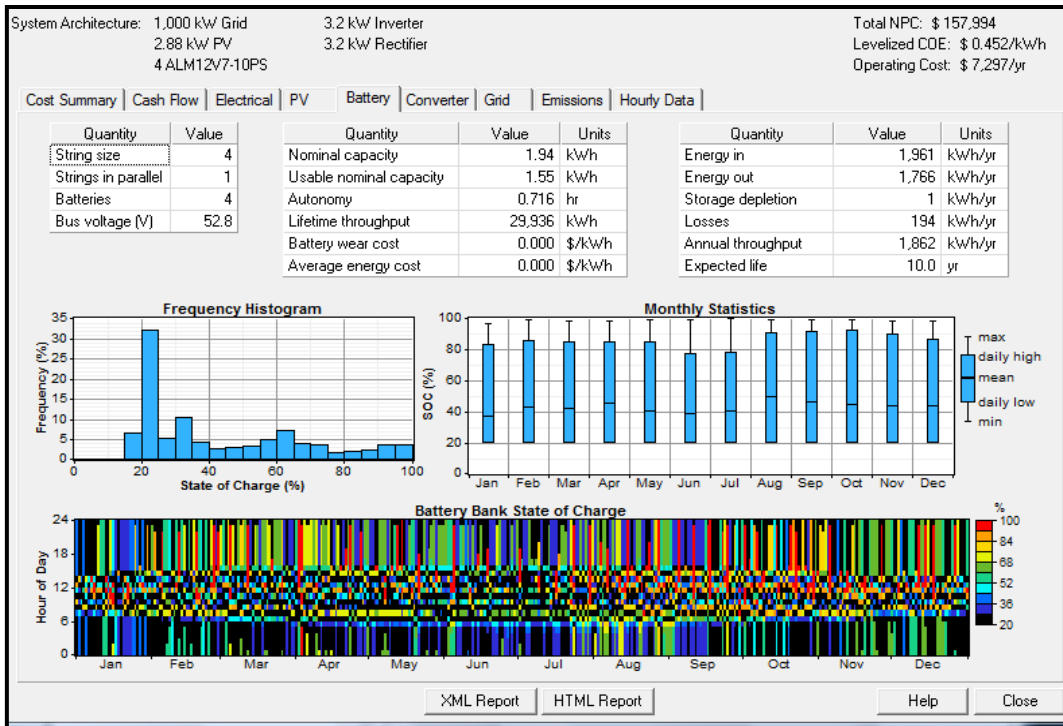Figure 40: Output for ALM12V7-10PN (Hydro-Quebec)

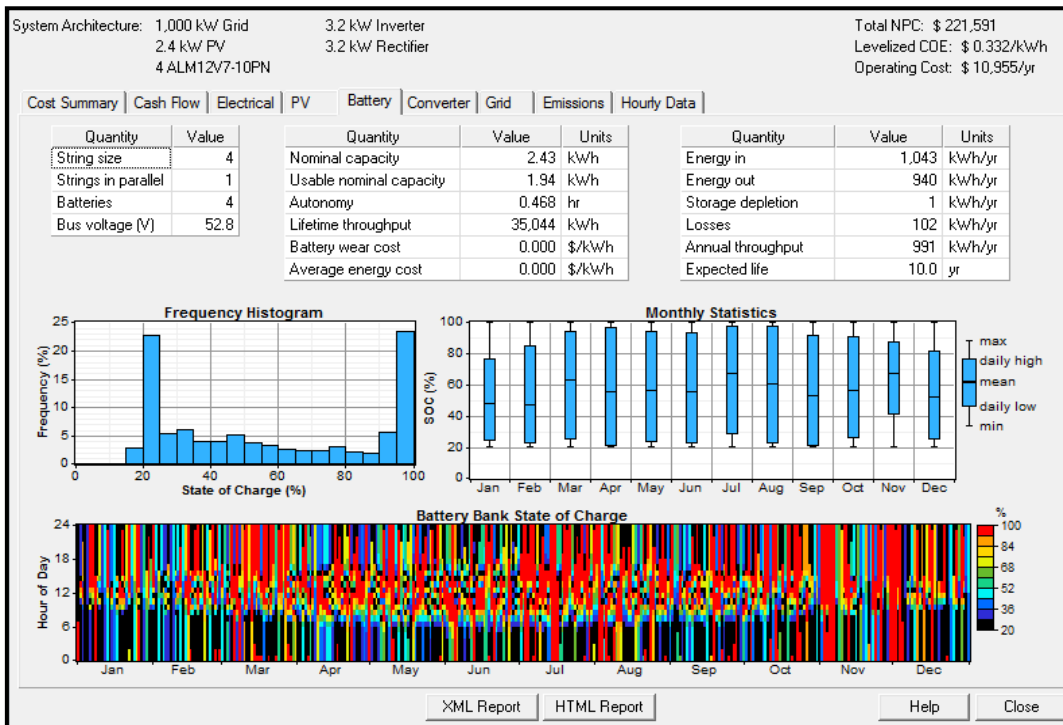**Figure 41: Output for ALM12V7-10PS (Hydro-Quebec)**



**Figure 42: Output for ALM12V7-10PN (Newcastle)**

**Figure 43: Output for ALM12V7-10PS (Newcastle)**

~ φ ~